PRO-ANGIOGENIC SELF-ASSEMBLING PEPTIDES

Jennifer Monique Carter

Thesis submitted to the faculty of
Virginia Polytechnic Institute and State University
in partial fulfillment of the requirements for the degree of

MASTER OF SCIENCE

In

Macromolecular Science and Engineering

John B. Matson, Chair
Judy S. Riffle
Tijana Z. Grove

April 17, 2015
Blacksburg, VA

Keywords: Angiogenesis, Self-assembling peptide, Hydrogen Sulfide

PRO-ANGIOGENIC SELF-ASSEMBLING PEPTIDES

Jennifer Monique Carter

ABSTRACT

Peptide amphiphiles (PAs), peptides that self-assemble into hydrogels with a nanofibrous network, are interesting biomaterials due to their biocompatibility and biodegradability. Self-assembling peptide-based materials include a wide range of peptide motifs that form one-dimensional nanostructures in aqueous solution. Two different PAs are considered in this M.S. thesis work: lipidated peptides, and gas-releasing peptides (GRPs). These biomaterials have been developed to function as potential therapeutics that promote the growth of new blood vessels. The analyses conducted on the lipidated peptides, which were designed to include a peptide sequence that promotes angiogenesis, include cytotoxicity, viability, and tube formation assays. The GRPs were designed to release H_2S, which is also capable of promoting angiogenesis. Several characteristic properties of the GRPs were analyzed, including morphology, mechanics, self-assembly, and gas release rates. Furthermore, cytotoxicity assays were conducted followed by the demonstration of gas uptake in endothelial cells.

DEDICATION

To my mother, Necia Henry, you are my motivation, without you this would not have possible. Just know that joy comes in the morning and troubles, they do not last always. I love you with all my heart.

ACKNOWLEDGEMENTS

Firstly, I would like to express gratitude to my committee members. I deeply appreciate my advisor Dr. John B. Matson for providing me such a great study opportunity, and support. His patient guidance and encouragement really helped promote my progress. I greatly acknowledge Virginia Tech and the Institute for Critical Technology and Applied Science (ICTAS) for providing funding and resources for this project, fund number JFC12-256.

I am extremely grateful for Dr. Riffle's encouragement and guidance during the years I spend at Virginia Tech. I thank Dr. Grove for providing me with various instructions and support.

Thank you to the Theus Group in the Virginia-Maryland Regional College of Veterinary Medicine at Virginia Tech, for their support and collaboration. I specially thank Thomas Brickler for the opportunity to work together, without you chapter two would not be possible.

I appreciate Jeffrey Foster and Yun Qian in my lab for their assistance on experiments and other laboratory work. I would also like to thank my other colleagues in Dr. Matson's group for their advice, assistance and friendship.

Finally, I would like to take this opportunity to express my heartfelt thanks to my beloved mother, godmother & father, my two brothers and dear friends for their support and encouragement.

TABLE OF CONTENTS

LIST OF FIGURES

LIST OF TABLES

CHAPTER 1: LITERATURE REVIEW

1.1 Introduction

Blood vessel formation is a highly complex process known as angiogenesis. This process involves an interaction between endothelial cells, their environment, and numerous signaling molecules.[1] Placentation, the female menstrual cycle and wound healing are examples of the physiological process of angiogenesis, which naturally occurs in adults. By maintaining a balance between the angiogenic signaling molecules, this process can be regulated. Dysregulation of these signaling molecules can be harmful to the human body. Inhibition of angiogenesis is a hallmark for several diseases including ischemic, inflammatory, and arterial disease, and chronic wounds.[2-3] Introducing angiogenic promoters to the body could help regulate blood vessel formation, allowing for the prevention or treatment of those diseases listed above. Current FDA approved treatments for these types of diseases and disorders include growth factor therapies,[4-5] tissue engineered products,[6] bioactive matrices,[7] mechanical systems,[8] and hyperbaric oxygen therapy.[9] These systems consist of expensive materials and therapeutic processes. The limited amount of angiogenic treatments available presents an opportunity to develop innovative therapeutic applications.

Biomaterials that promote angiogenesis have shown promising results in animal models, but their ability to produce beneficial outcomes, from bench-to-bedside, has been limited. While growth factors are currently utilized in these therapies, their shortcomings include short half-

lives in vivo, high cost, and immunogenicity.[10] To overcome these disadvantages peptide fragments that mimic growth factors (GFs) are under investigation due to their ease of synthesis and reduced immune response. Such peptide fragments contain the important amino acid motifs found in GFs to produce the desire physiological response. However, peptide fragments are quickly metabolized and have a short retention time at the injection site.[11] Due to the drawbacks in current biomaterials used as angiogenic therapeutics, designing such a material with higher efficiency is desirable.

In addition to growth factors, gasotransmitters also play an essential role in vascular activity.[12] Gasotransmitters are gaseous molecules that are produced endogenously and contribute to several physiological and pathological functions in the body. These molecules include carbon monoxide, nitric oxide, and hydrogen sulfide. Several gas-releasing molecules (GRMs) have been synthesized for exogenous delivery for potential medical applications.

Incorporating peptide fragments or GRMs into biomaterials that self-assemble in aqueous solutions, forming entangled nanofibers, may increase retention time at the injection site compared with bare peptide fragments or small- molecule GRMs. Amphiphilic molecules have a hydrophilic (polar) and a hydrophobic (nonpolar) component which allows them to aggregate in aqueous solutions. Self-assembling peptides (typically peptide amphiphiles (PAs) or aromatic peptides) used as biomaterials for regenerative medicine have emerged due to several important characteristic, such as mimicking large proteins, incorporating bioactive epitopes and biocompatibility.[13-14] PAs also possess the morphology that resembles the fibrous nature of the extracellular matrix (ECM), allowing for cellular recognition of the network. Additionally, GRMs have been incorporated into the structural design of PAs, thus producing gas releasing peptides (GRPs). [15] Due to the tunable design of GRPs, they allow for site-specific delivery of

gasotransmitters at physiologically relevant rates. In this research, we aim to synthesize PAs and GRPs that self-assemble into hydrogel networks. These peptides will be studied for their potential use as injectable biomaterials to treat traumatic brain injury (TBI) through angiogenic therapy.

1.2 Traumatic Brain Injury

In the United States, more than 2.4 million emergency department visits, hospitalizations, or deaths are related to TBI. Approximately 5.3 million people who have endured TBI are facing permanent damage, including long-tern cognitive and psychological impairments.[16] The collective annual cost of treating TBI in the United States now approaches $76.5 billion.[17] TBI refers to an external impact force to the head causing brain dysfunctions. These dysfunctions result from either closed injuries such as a bump, blow, or jolt to the head, or penetrating head injuries. Understanding that the brain defines who we are as human beings, a brain injury can affect all aspects of our lives, including our personality, and physical and mental ability.

Secondary injury evolves over time after the initial trauma, resulting in fatality or severe disabilities due to neuro destruction. Trauma, ischemia or a reperfusion injury causes chemical disruption on the blood – brain barrier, edema and neural death.[18] Legions may form in the cerebrum from such injuries, which will also contribute to secondary TBI.

Despite decades of research, no treatment has been shown to improve secondary TBI. To minimize secondary injury and life support, patients undergo acute treatments, which consist of a ventilator and brain surgery. Drug induced comas are also performed to minimize secondary injury, as well as agitation.[16] Patients are usually provided with anti-inflammatory drugs and pain

and behavioral medication. Therefore, there exists a definite need for the development of TBI treatments that promote both the repair and regeneration of injured brain tissue with functional recovery.

In early 2014, ProTECT (Progesterone for Traumatic brain injury--Experimental Clinical Treatment) phase III clinical trials were discontinued.[19] The trial was designed to determine if progesterone, a steroid with neuroprotective properties in animal models containing brain injury, could be beneficial in treating patients with moderate to severe acute traumatic brain injury.[20] The failure of this clinical trial compels a need to construct a better therapy for TBI.

Earlier strategies to improve brain function after TBI used a neurogenesis approach. However, the development of new neurons in the brain depends on newly formed blood vessels to aid their metabolic and trophic needs. Gage and associates were the first to show that adult neurogenesis occurs within an angiogenic niche.[21] The observed neural and angioblast clusters were surrounded by vascular endothelial growth factor (VEGF), a critical signaling proteins for angiogenesis processes, suggesting that neurogenesis shared or was codependent with endothelial signaling processes. Based on their data, neurogenesis occurs within the context of angiogenesis.[21] The adult brain vascular system is stable unless pathological conditions occur, including injury. Investigations have also shown that the expression of VEGF increases in the brain after TBI, intensifying cerebral angiogenesis.[22-24]

Therapeutic angiogenesis, a more recent approach for fighting diseases, such as diabetic foot ulcers,[4, 25-26] and surgical and trauma wounds,[7] stimulates blood vessel formation to reconstruct the form and function of impaired tissues. Utilizing therapeutic angiogenesis for TBI may provide promising opportunities for brain functional recovery and reduce possible resulting

disorders.[24, 27] Pro-angiogenic therapies are needed to prevent or treat diseases related to the inhibition of blood vessel formation.

According to the Angiogenesis Foundation, there are currently three major areas where angiogenic therapies are used: these include chronic wounds, peripheral arterial disease, and ischemic heart disease. In these therapies, the goal is to stimulate blood vessel formation by restoring the form and function of injured tissues. Several GFs have been used as a treatment for these diseases. Becaplermin, a topical recombinant human form of platelet-derived growth factor (PDGF-B) was approved by the Food and Drug Administration (FDA) in 1997, and is used for the treatment of diabetic foot ulcers.[4, 25-26] OASIS® Wound Matrix, a commonly used bioactive dressing, is an ECM product derived from the small intestinal submucosa of pigs.[7] It received FDA approval in 2000 for the treatment of several types of ulcers, surgical and trauma wounds. This matrix consists primarily of collagen-based ECM but also contains hyaluronic acid, proteoglycans, fibronectin, fibroblast growth factor-2 and transforming growth factor β.[7] The beneficial outcomes of the mentioned therapies inspired us to develop angiogenic therapeutics to treat acute TBI.

1.3 The Process of Angiogenesis

Angiogenesis is the essential process of blood vessel formation from pre-existing blood vessels. After the embryo undergoes vasculogenesis, the development of a *de novo* primitive vascular network, capillaries form extensively by splitting (intussusceptive) or sprouting angiogenesis.[28-29] *In vivo*, intussusceptive angiogenesis occurs when endothelial cells (ECs) proliferate within the mother blood vessel, producing a lumen that splits by transcapillary pillars

producing two sister blood vessels. Folkman and Ausprunk provided the first description of sprouting angiogenesis, as illustrated in Figure 1.[30] Activation of angiogenesis occurs by VEGF binding to VEGF-R. Vascular smooth muscle cell proliferation is inhibited, followed by the proteolytic degradation of the basement membrane by matrix metallopropteinases (MMPs) and urokinase plasminogen activators (uPAR). Endothelial cells then proliferate and migrate toward growth factors. These newly developed cells begin to elongate and arrange into a tube. Stabilization of the neocapillaries occurs once the basement membrane is reconstructed, and the immature vessels are covered by pericytes and smooth muscle cells.[31-33] In adults, blood vessel formation is ephemeral, only observed during specific physiological conditions, including placentation, the female menstrual cycle,[32] and wound healing.

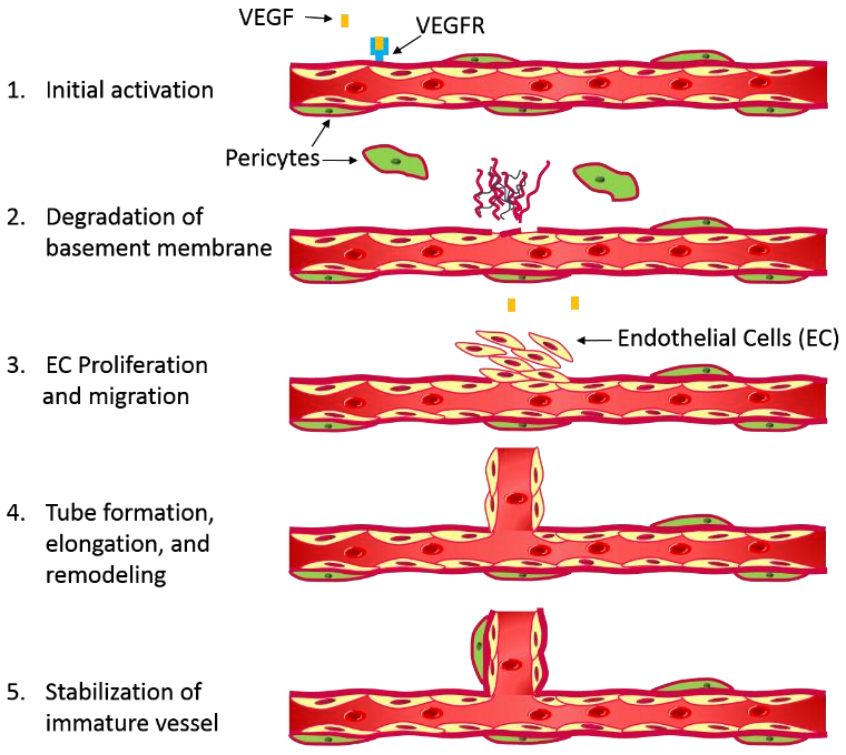

Figure 1.1: The process of intussusceptive Angiogenesis

The activity of angiogenesis plays a critical role in the health of human beings. Angiogenic signaling molecules that either inhibit or promote blood vessel formation regulate this activity. Physiologically, the balance of angiogenic promoters and inhibitors is highly regulated via "on" and "off" regulatory keys, such as angiogenic growth factors and endogenous angiogenic inhibitors, respectively.[34] Dysregulation of these keys contributes to pathological diseases. During up-regulation of angiogenesis certain pathological conditions, such as cancer, atherosclerosis, and diabetic retinopathy, are triggers.[1] Down-regulation of angiogenesis contributes to ischemia, coronary artery disease (CAD), cardiac failure, and tissue injury. To prevent unwanted outcomes associated with blood vessel formation, it is important for the body to regulate the signaling molecules related to the processes of angiogenesis.

1.4 Angiogenesis Signaling Molecules

While the angiogenic molecules outlined in Table 1 are described in detail in several reviews, [35-49] we wish to focus on the gasotransmitters and peptide fragments found in different proteins, specifically H_2S, and SVVYGLR, respectively. VEGF, FGF, and PDGF have been administrated as angiogenic therapies and will also be explained.

	References
Angiogenin	35
Angiopoientins (Ang-1)	36
Cyclooxygenase-2	37
Ephrins	38
Fibroblast growth factors (family)	39
Follistatin	40
Gasotransmitters – Carbon monoxide, Nitric Oxide, Hydrogen Sulfide	41-43
Granulocyte colony-stimulating factor (G-CSF)	44
Hepatocyte growth factor/scatter factor – HGF/SF	45
Platelet-derived growth factor – PDGF	46
Integrins	47
Transforming growth factors TGF -α & TGF-β	48
Vascular endothelial growth factor (family)	49

Table 1.1: A list of several endogenous angiogenic promoters

1.4.1 Vascular Endothelial Growth Factors

Vascular endothelial growth factors (VEGF) are critical signaling molecules for angiogenesis processes. VEGF is a potent mitogen for endothelial cells. The VEGF family consist of seven glycoproteins, VEGF-A, VEGF-B, VEGF-C, VEGF-D, VEGF-E, VEGF-F and placental growth factor PLGF.[50] All of these members interact with VEGF receptors, known as transmembrane tyrosine kinases. These receptors are identified as VEGFR I, II, and III, and the neuropilins (NP I, and II).[51] The binding of VEGF to its receptor leads to receptor dimerization by autophosphorylation. This interaction initiates a cascade of protein formulation and cell signaling through intracellular receptor tyrosine kinases, resulting in several biological effects.

VEGF – receptor (VEGF-R) binding is specific, and the biological effects depend on the particular interaction.

VEGF-A and its receptors are the best-characterized signaling pathways in the area of developmental angiogenesis.[52] This GF also acts as a neuroprotectent and induces neurogenesis.[53] VEGF-A, referred as VEGF, has been identified as an effective mitogen that is a major regulator for the promotion of endothelial cell proliferation, vessel sprouting and tube formation.[54] There are at least eight known human isoforms ($VEGF_{121}$, $VEGF_{145}$, $VEGF_{162}$, $VEGF_{165}$, $VEGF_{165b}$, $VEGF_{183}$, $VEGF_{189}$, and $VEGF_{206}$) corresponding to the number of amino acids. Loss of a single VEGF-A allele results in embryonic lethality.[55] This pathway also has an essential role in reproductive, bone, and tumor angiogenesis.[56-57] VEGF-A interacts with VEGFR-1, VEGFR-2, NP-1 and NP-2. Pro-angiogenic and permeability-enhancing effects are mainly mediated through the binding of VEGF with VEGFR-2. The binding of VEGF-1 is more complex, but reports show that it is involved in the processes of inducing MMPs.[58]

1.4.2 Fibroblast Growth Factors

In contrast to VEGF, which is specific for vascular cell growth, the FGF family contains strong mitogens that have an influence on many other cell types as well. These growth factors are also associated with several disorders. There are 23 FGFs (FGF1-23), that bind and activate four tyrosine kinase FGF receptors (FGFR1-4).[39] In particular, FGF-1 and FGF-2 are important for stimulating angiogenesis during wound healing.[46] FGF promotes cell proliferation, angiogenesis and improves perfusion in ischemic limbs, and wounds.[59-60]

1.4.3 Platelet-derived growth factor

Another important signaling molecule involved in the processes of blood vessel formation is PDGF with its receptor PDGFR-β. [61] PDGF can be secreted from several cell types, as either a homo- or heterodimer. Vascular maturation by recruiting smooth muscles cells and pericytes is mediated by PDGF-β signaling.[62]

1.4.4 Protein Fragments

As mentioned above, angiogenesis is regulated by various growth factors, as listed in Table 1. Although several growth factors are used for angiogenic therapies,[4, 25-26, 46, 63] they are immunogenic and expensive due to their high molecular weights. Contrary to using large proteins, small peptide sequences containing the cell-binding motif of the native protein can be used to trigger its innate bioactive responses. The advantages of protein motifs include ease of synthesis, cost efficiency, and low immune responses. Several small peptide sequences that have shown improvement of EC activity include Arg-Gly-Asp (RGD),[64] Tyr-Ile-Gly-Ser-Arg (YIGSR),[65-66] and Ile-Lys-Val-Ala-Val (IKVAV).[67]

RDG, a tripeptide motif, was originally identified in fibronectin[68] but has since been found in numerous other proteins such as collagen,[69-70] osteopontin,[71-72] vitronectin,[73] and tenascin C[74]. The RGD sequence is the ligand for integrin-mediated cell adhesion, which involves a cascade of four overlapped reactions important for transmitting signals related to cell behavior and the cell cycle. These reactions include cell attachment, cell spreading, actin-

skeleton formation, and focal-adhesion formation.[75] Since the identification of RGD, it has been investigated extensively.[64, 76-77]

Laminin, a ~810 kDa extracellular matrix protein, is a basement membrane component that has a multi-domain structure with various functions. Research has identified the peptide, YIGSR as a key sequence for cell attachment, and spreading.[65-66] Several reports have demonstrated YIGSR as a component to improve endothelialization.[78-79] IKVAV, another peptide motif found in laminin, promotes neurite outgrowth, plasminogen, and cell adhesion.[67]

In the past decade, the protein fragment, Ser-Val-Val-Tyr-Gly-Leu-Arg (SVVYGLR), found adjacent to Arg-Gly-Asp (RGD) in osteopontin, has been identified as a peptide involved in angiogenesis.[80] This protein is present in various areas such as bone tissue, kidney, brain, and skin. Osteopontin participates in the bone metabolism and also mediates inflammatory responses and angiogenesis.[81] Following thrombin cleavage, SVVYGLR binds to integrin $\alpha_9\beta_1$, enhancing cell migration and proliferation necessary for tissue remodeling.[80] SVVYGLR promotes endothelial cell activities including adhesion, proliferation, migration, and tube formation.[82-83]

Unfortunately, protein motifs, as a single small molecule have a short circulatory half-life, poor metabolic stability, and possible immune responses.[84]

1.4.5 Gasotransmitters

The angiogenesis signaling molecules listed above all have the ability to influence EC activity or blood vessel formation. Introducing gaseous molecules could provide an innovative approach for angiogenesis therapeutics. Gasotransmitters are gaseous signaling molecules that contribute to the regulation of physiological and pathological functions in the body.[85-86]

Currently, there are three known gasotransmitters: carbon monoxide (CO), nitric oxide (NO) and hydrogen sulfide (H_2S), all of which are endogenously produced. These gases were originally known for their reputation as toxic substances and environmental hazards. CO, known as a silent killer, is an excessive atmospheric pollutant, originating slowly from natural sources but more abundantly from industrial and technological activity.[87] NO, also an excessive atmospheric pollutant, is the source of the polluting NOx, emanating from combustion reactions and industrial manufacturing. H_2S, a main focus in this research, is best known for its rotten egg smell and its toxicity. However, at appropriate concentrations these gases are essential signaling molecules. Interestingly, all three gasotransmitters are transported through cell membranes without any regulatory transports via a passive diffusion mechanism.[88] Despite the significant dipole moment and large polarization of H_2S, it is solvated and permeates membranes like a hydrophobic solute.

1.4.5.1 Carbon Monoxide

CO is generated when heme undergoes degradation via oxidation by heme oxygenase.[86] Once the heme iron is released as a ferrous cation (Fe^{2+}), the α-methene bridge carbon is eliminated as CO. Aside from the production of CO during heme oxidation, biliverdin is generated and is reduced to bilirubin by NADPH.[89] Although all of the products generated during heme degradation have a biological affect, it has been shown that various biological activities, such as cardioprotection,[90] anti-inflammatory effects,[91] and anti-apoptosis properties,[92] are related to CO regulation.

1.4.5.2 Nitric Oxide

Physiological NO arises from the conversion of L-arginine to L-citrulline stimulated by nitric oxide synthase (NOS) enzymes. There are three isozymes of NOS that are associated with NO production; neuronal NOS (nNOS) found in neuronal cells and skeletal muscle; endothelial NOS (eNOS) found in endothelial and epithelial cells; and inducible NOS (iNOS), found throughout the body mainly in cytokine-induced cells.[86, 93] Due to their ubiquitous expression, NOS enzymes have a wide variety of physiological effects such as proliferation and apoptosis of cells, vascular toning,[94] cell relaxation,[95] neurotransmittion,[96] and anti-thrombogenicity[41].

1.4.5.3 Hydrogen Sulfide

Hydrogen sulfide (H_2S), known for its unpleasant rotten egg smell, is classified as the third gasotransmitter, subsequent to NO and CO. H_2S was initially considered as a highly toxic gas existing only as a hazard to the environment.[97] This negative notion was reassessed after the recognition that H_2S acts as a neurotransmitter.[98] The discovery that H_2S is enzymatically produced in the body initiated the necessities to investigate the importance of H_2S in physiological conditions. Endogenously, H_2S is produced via several enzymatic processes. The physiological mechanisms of H_2S production have been well explained by Paul and Snyder, and is illustrated in Fig. 2.[99] Cystathionine-β-synthase (CBS) and cystathionine-γ-lyase (CSE) are pyridoxal-5′-phosphate (PLP)-dependent enzymes that metabolize L-cysteine to generate H_2S.[100] Also, 3-mercaptopyruvate sulfurtransferase (MST), accompanied by cysteine (aspartate) aminotransferase (AAT) generates H_2S from cysteine and α-ketoglutarate.[101]

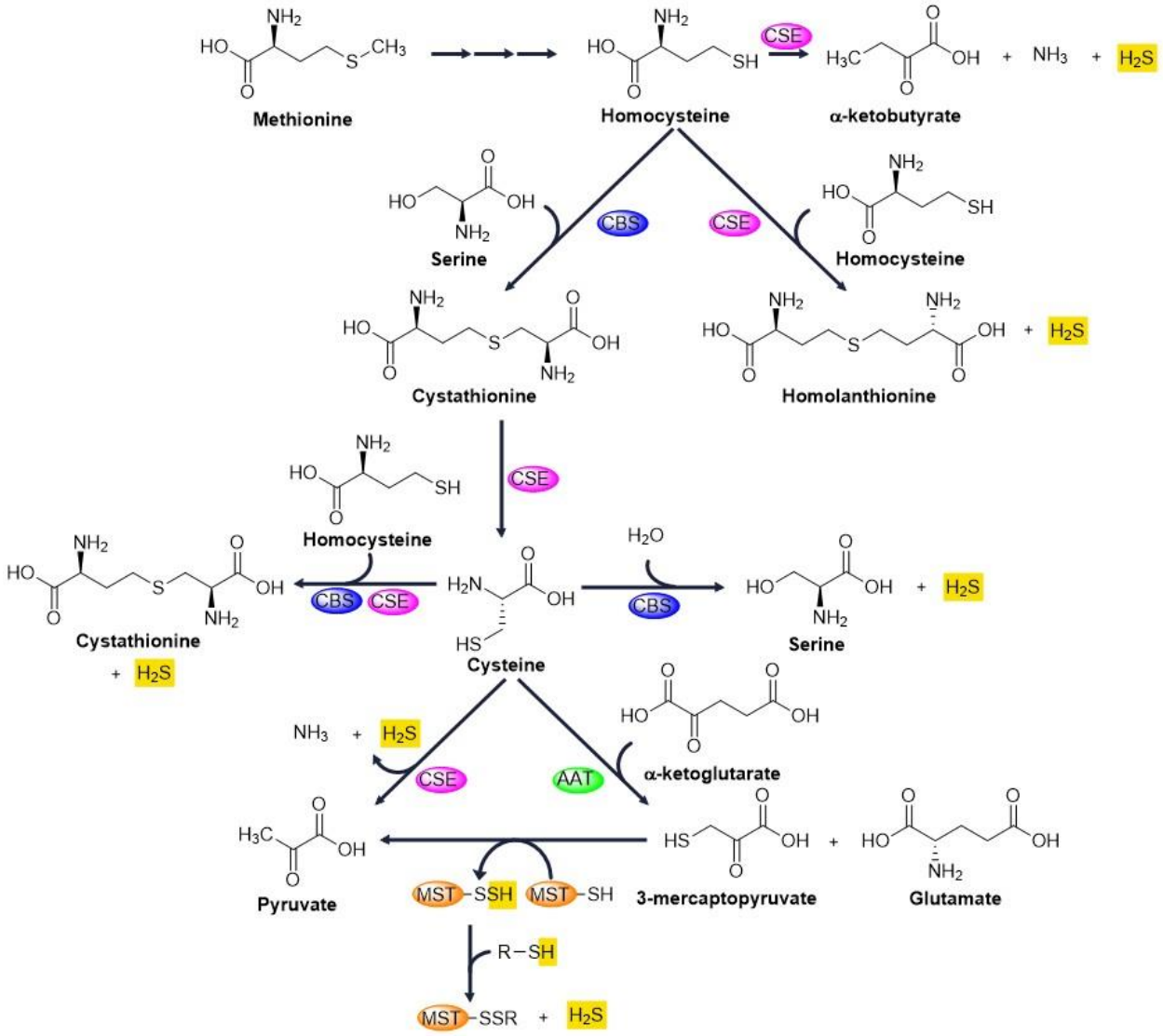

Figure 1.2: Mechanism of physiological H_2S production in mammals. Adapted[99]

As shown in Fig. 2, H_2S (highlighted in yellow) is produced in several ways. Initially, homocysteine, derived from methionine, is linked with serine to generate cystathionine by CBS. Then CSE catalyzes the γ-elimination reaction, which degrades cystathionine into cysteine.[102] Cysteine can then be converted into H_2S, pyruvate and ammonia by CSE. This enzyme also generates metabolites such as α-ketobutyrate, homolanthionine, and cystathionine and depending

on the reaction. α-Ketobutyrate is produced from homocysteine; homolanthionine is produced from 2 equivalents of homocysteine; and cystathionine is produced when cysteine combines with homocysteine, all modulated by CSE. Cystathionine and H_2S are also produced from cysteine and homocysteine when catalyzed by CBS. H_2S and serine are generated when cysteine reacts H_2O, catalyzed by CBS.[99]

MST in conjunction with AAT mediates a third H_2S generating pathway. CBS was previously thought to be the dominant H_2S generating enzyme in the brain, but in the brain of CBS-knockout mice, H_2S levels are similar to those of the wild-type mice, indicating that there must be another enzyme that helps produce H_2S.[103] Kimura and colleagues conducted a study showing that MST generates H_2S from cysteine in combination with AAT. First, 3-mercaptopyruvate and glutamate are formed from cysteine and α-ketobutyrate by AAT. The thiol group on the 3-mercaptopyruvate links to MST at the cysteine residue located in the active site. The storage of H_2S occurs through this formation, in which sulfane sulfur binds to proteins or cysteine residues via a divalent sulfur bond.[103] From here, H_2S is generated in the presence of a reductant, such as glutathione.

While all three enzymes catalyze the production of H_2S, their concentrations, distributions, and efficiencies are regulated by tissue specific imperative production of H_2S. However H_2S is generated, it is an endogenous gas that is involved in many physiological processes.

H_2S participates in several signaling pathways, influencing tissue specific functions. Importantly, H_2S induces vascular relaxation and promotes angiogenesis.[104] These occurs during the direct activation of VEGFR-2 caused by H_2S reduction about the receptors disulfide bonds.[105] H_2S also acts as a neurotransmitter, anti-inflammatory, and antioxidant.[106-107] In mammals, the

concentration of H_2S depends on the specific organ of interest. The investigation of H_2S is continuously evolving for its use as therapeutic applications.

Recently, it has been shown that a number of diseases are related to the dysregulation of endogenous H_2S. In earlier studies, H_2S gas, or salts, Na_2S and NaHS, were used to determine the physiological and pathological effects of H_2S. H_2S gas has limited benefits as a therapeutic agent due to difficulties of controlling its concentrations, which might cause toxicity. H_2S salts are rapidly oxidized by O_2, resulting in a short half-life, and releasing H_2S rapidly. This is problematic because *in vivo* H_2S is generated in a slow and continuous process.[108]

As a result, an increasing number of H_2S donors, either natural or synthetic, have been developed and evaluated for potential therapeutic use. Among those are compounds incorporating various functional groups including, diallyl di-trisulfide, dithiolethione, thioamide, aminothiol, isothiocyanate, derivatives of Lawesson's reagent, and aroylthioamides.[100, 108-109] Most recently, *S*-aroylthiooximes (SATOs) have been developed for use as H_2S donors.[110] Similar to *N*-(benzoylthio)benzamides and arylthioamides[109], SATOs are thiol-activated H_2S donors. SATO molecules synthesized from either an aldehyde or ketone are relatively stable in physiological conditions.

However, these low molecular weight molecules have inherent pharmacokinetic problems and therefore do not fully mimic endogenous H_2S. To overcome these shortcomings, it is essential that H_2S donors be constructed to have long half-lives, releasing and promoting H_2S at a sustained and controlled rate. Recently, a PEGylated dithiolethione conjugate was synthesized as a polymeric H_2S donor, to reduce the risk of cytotoxicity caused by the small molecule H_2S donor.[111] In this report sustained and controlled release of H_2S was not addressed. In another recent report, an array of functionalized methacrylate polymers were post modified

with SATO chemistry, classifying them as H_2S releasing polymers.[112] Incorporating polymers with the SATO functionality allowed for controlled release of H_2S. From these findings, we hypothesize that SATO has the potential to be incorporated into a more biocompatible system, such as a self-assembling peptide, for local delivery of H_2S.

1.5 Research approach

In this research, we aim to synthesize lipidated peptides and H_2S-releasing peptides that promote angiogenesis for TBI treatments. Both systems rely on peptide self-assembly resulting in nanofiber hydrogels that mimic the extracellular matrix (ECM).

1.5.1 Supramolecular Peptide-Based Gelators

Supramolecular hydrogels are ideal drug delivery systems. Their size and surface properties can be manipulated to avoid rapid clearance by phagocytic cells, allowing both passive and active drug targeting. Additionally, they can control and sustain drug release at the target site, improving therapeutic efficacy and reducing side effects. Drug loading is relatively high and may be achieved without chemical reactions; this is an important factor for preserving the drug activity. Self-assembled nanofibers are a type of supramolecular polymer made from building blocks connected via non-covalent interactions that result in self-assembly or aggregation of those blocks. In response to some stimuli, simultaneous organization of the building block will occur. The majority of self-assembling peptides possess amphiphilic characteristics, conjoining a hydrophobic or aromatic component to a hydrophilic component.

Although the interactions keeping the nanostructures together are weak, including electrostatic interactions, hydrogen bonds, hydrophobic and hydrophilic interactions, π-π stacking, or van der Waals interactions, the collective interactions produce structurally and chemically stable aggregates. Proteins utilize this concept frequently in nature; for example, actin monomers, in the cell cytoskeleton, can form filaments and depolymerize dynamically.

The structural design of peptide amphiphiles (PAs) was first reported in 1995 by Tirrell and co-workers.[113] In their report, a dialkyl tail was conjugated onto a collagen peptide motif resulting in the assembly of a monolayer at the air-water interface. Such molecules have also been extensively investigated in the Stupp laboratory.[114] This type of PA consists of a peptide sequence appended to a single alkyl tail. In addition to the alkyl tail, three structural regions of the peptide component are typical. Region 1 is a short peptide sequence with high β-sheet propensity. Region 2 contains charged amino acids to enhance water solubility and for the design of pH and salt-responsive nanostructures and networks. The third region consists of a bioactive peptide, an epitope that promote cellular response by interacting with receptors on the surface of cell membranes.[13, 114] Although, all regions play a major role in the final properties of the PA assembly, the β-sheet and the hydrophobic regions are most pertinent to the strength of the nanostructures.

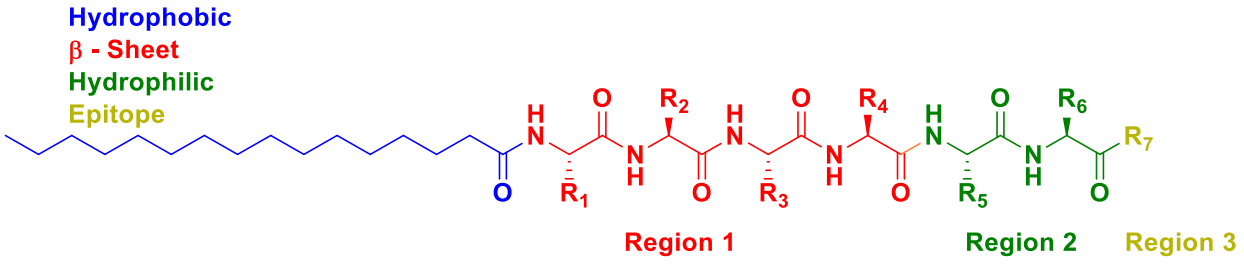

Figure 1.3: General Structure of Self-assembling Peptide Amphiphiles containing a hydrophobic tail appended to a peptide sequence that has three distinct regions.

Direct self-assembly of PA can also be achieved by incorporating an aromatic moiety. In this case self-assembly is driven by the directionality associated with the resultant π-π stacking interactions. First reported by Reches and Gazit, was the self-assembly of aromatic dipeptides into nanotubes and vesicles.[115] The Xu group then discovered that self-assembly can also be driven by incorporating a fluorenylmethoxycarbamyl (Fmoc) group, which aggregates through hydrophobic and π-π stacking effects. Following this discovery, the Ulijn group investigated Fmoc-dipeptide hydrogels as biomaterials for cell culture and developed a library of seven molecules to tune their relative hydrophobicity.[116-117]

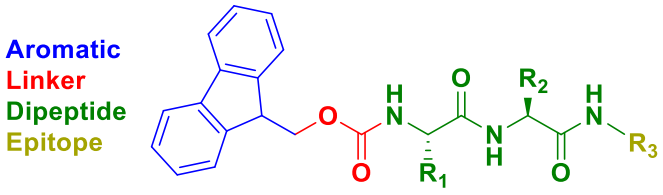

Figure 1.4: General structure of aromatic peptide amphiphiles with the Fmoc moiety

In nature, proteins have well defined α-helices or β-sheets, which comprise their secondary structures and tertiary structures. The conformation of a peptide sequence present in PAs strongly depends on the amino acids' propensity for certain secondary structures. After the confirmation of the myoglobin protein structure, via X-ray crystallography, interest in the amino acid secondary structure preference grew.[118] Many articles have been published in regards to the essential amino acids and their propensity to form α-helices, β-sheets, or random coils. Levitt analyzed this propensity using a basic method by counting the number of times an aa occurs in a known protein structure.[119] The occurrence is given by a modified binomial probability distribution equation, shown below in Fig. 4. Where *n* is the number of times aa *i* occurs in the

protein structure *j*, depending on the total number of aa N_i, in the total number of protein structures N_i, of all proteins studied *N*.

$$P_{ij} = \left(\frac{n_{ij}}{N_i}\right) / \left(\frac{N_j}{N}\right)$$

Figure 1.5: The modified binomial probability distribution equation used to calculate the AA propensity for secondary structure.

Based on their findings, Val, Ile, Thr, Phe, Tyr, and Trp all had high β-sheet propensities.[119] In another report, a systematic analysis of the interactions of parallel β-sheets was carried out to analyze amino acid propensities and their pair correlations.[120] The amino acids with the highest self-pair occurrence were Ala, Ile, and Val. Based on this data, Ile, Ala and Val are good candidates for the β-sheet region of LPs. This understanding inspired the peptide sequence used in this work.

Self-assembling peptide-based materials that release NO or CO have been studied in the form of films or hydrogels for potential therapeutic applications. A self-assembling PA was synthesized and designed to prolong CO delivery *in vitro* to address the rapid depletion of small molecule CO-releasers.[15] The CO-releasing PA contained a C_{16} alkyl tail appended to the β-sheet peptide sequence, $V_3A_3E_3$. The CO-releasing molecule (CORM), $[Ru(CO)_3Cl_2]_2$ was attached to the side chain of a glutamic acid residue affording the CO-releasing PA. When analyzing the CO release from the PA, the PA gel had an 8-fold increase in the release half-life when compared to the CORM and the PA in solution. From this report, it is evident that PA hydrogels have potential as therapeutic applications with reduced dose load and local delivery of gasotransmitters.

1.5.2 Peptide Synthesis

Solid phase peptide synthesis (SPPS), pioneered by Merrifield, is the most common methodology used to synthesize peptides. This technique involves resin beads containing functionalized linkers, e.g., amine or carboxylic acid groups, which act as a solid support for peptide growth. The resin bead allows separation of the growing insoluble peptide from excess reagents and side products by filtration and washing. The functional groups on the side chains associated with the amino acid residues must be temporarily protected during all reaction steps to maintain peptide growth along the backbone. The temporary protecting groups are usually either fluorenylmethyloxycarbonyl (Fmoc) or tert-butyloxycarbonyl (Boc), which is how the two main strategies for SPPS are classified (Boc and Fmoc chemistry). Their structures are provided in Fig. 5.

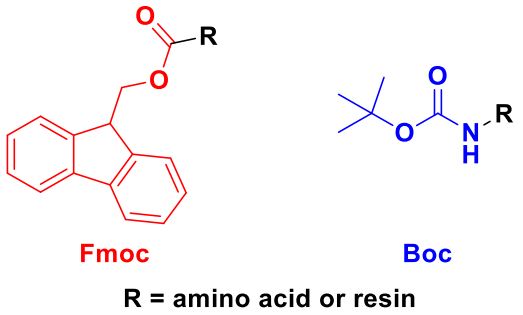

Figure 1.6: Two common SPPS Protecting Groups

When Merrifield invented SPPS in 1963, tBoc chemistry was the primary method used.[121] To remove Boc from the α-nitrogen of the growing peptide chain, acidic conditions are used (usually neat TFA). Removal of side-chain protecting groups and the peptide from the resin at the end of the synthesis is achieved by incubating in hydrofluoric acid (which can be dangerous); for this reason Boc chemistry is generally disfavored. The elimination of HF can be

achieved by using Fmoc chemistry. The Fmoc method is based upon an orthogonal protecting group strategy, a secondary amine is used for deprotection and TFA is used for cleavage, eliminating the use of HF. Therefore, Fmoc chemistry is used in this research.

The mechanism for SPPS via Fmoc chemistry is illustrated in Scheme 1. The desired peptide sequence is assembled in a linear fashion using the C to N strategy, from the C-terminus to the N-terminus. Rink amide resin is a polystyrene bead that contains an Fmoc amine functionalized linker. The amine is deprotected with a base followed by the addition of the first amino acid. The N-protected C-terminal amino-acid residue is coupled via its carboxyl group to the free amino resin to yield an amide linked peptide that will ultimately produce a C-terminal amide peptide. The next amino acid is coupled to the deprotected amino acid anchored to the resin. The peptide sequence is synthesized by these repetitive cycles of α-N deprotection and amino acid coupling reactions. In this research, after the desired peptide sequence is synthesized manually or on an automated peptide synthesizer, either palmitic acid, or the linker acetylbenzoic acid (ketone linker) or 4-formylbenzoic acid (aldehyde linker) is coupled to the N-terminal to form a LP or GRP, respectively. Once the sequence is complete, peptide cleavage from the resin and deprotection of side chain protecting groups is done using a trifluoroacetic acid (TFA) cleavage solution.

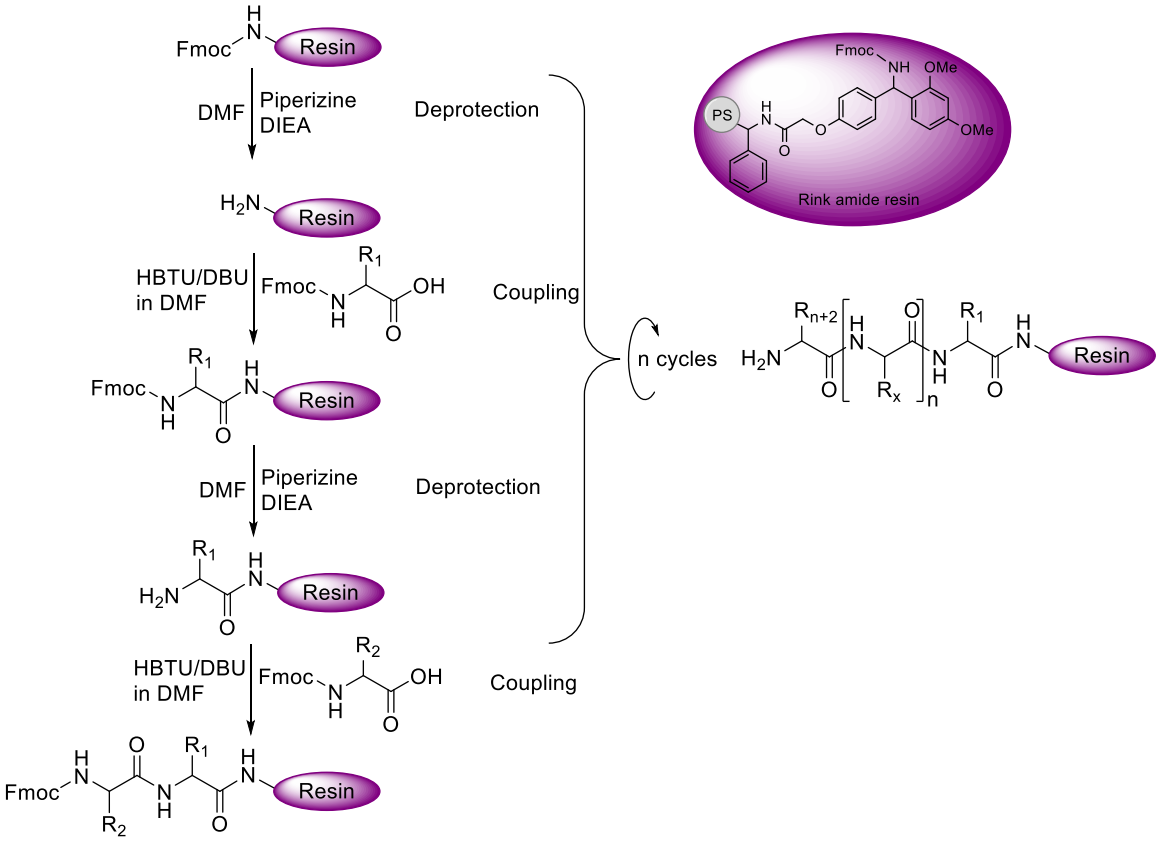

Figure 1.7: The mechanism of SPPS via Fmoc chemistry

1.5.3 Lipidated Peptides

The peptide motif SVVYGLR, adjacent to RGD in OPN, has been shown to promote EC tube formation. LPs self-assemble into nanofibers, which have potential as injectable local delivery therapeutics. In hopes of providing more bioactivity to the LPs, preliminary investigations were done to replace the traditional palmitic acid tail with different bioactive lipids. We hypothesize that LPs containing the epitope SVVYGLR with a bioactive carbon chain have potential use as angiogenesis-promoting gels.

1.5.4 Gas Releasing Peptides

Szabo and associates have reported the roles of exogenous and endogenous H_2S during angiogenesis, demonstrating both endothelial cell proliferation and blood vessel formation.[104] After exposing human umbilical vein endothelial cells (HUVECs) to H_2S (60 μM) there was a 2-fold increase in cell proliferation.[104] From this data, we hypothesize that H_2S-releasing biomaterials have potential use as pro-angiogenic therapeutics. As mentioned above, H_2S donors that provide a controlled release rate are likely to be ideal for promoting angiogenesis. Utilizing self-assembling peptides as H_2S donors could provide a controlled release rate of H_2S from the hydrogel. When H_2S is released at a controlled rate, the exogenous production and level of H_2S will be similar to that of endogenously produced H_2S.

1.6 Thesis Overview

The research presented in this thesis focuses on the development of two self-assembling peptides that have potential use as angiogenic therapeutics. This document explains the research conducted and the results that support the conclusions. In chapter 2, the synthesis of an LP containing the SVVYGLR motif will be introduced. Preliminary work on this LP will be presented which includes the experimental procedures used to analyze the cytotoxicity, viability, and tube-formation assays. Chapter 3 discusses the synthesis of H_2S-releasing peptides and the experimental procedures, results and discussions are provided. The conclusions of the research and suggestions on directions for future work in this research area are provided in Chapter 4.

CHAPTER 2: SVVYGLR SELF-ASSEMBLING PEPTIDE

2.1 Introduction

Traumatic brain injury (TBI) is a leading cause of disabilities and deaths in the United States. Currently there are no treatments to improve acute TBI, compelling a need to develop new therapeutic approaches. Supramolecular hydrogels are ideal drug delivery systems for tissue engineering therapeutics due to their biocompatibility, bioactivity, and potential to stimulate function. For effective tissue regeneration, new blood vessel formation is necessary to deliver nutrients to cells for survival. Old age,[122] diabetes,[123] endothelial dysfunction, chronic wounds,[124] and trauma[21, 27] can impair the processes of naturally occurring angiogenesis. Introducing exogenous angiogenic molecules can help stimulate blood vessel formation in instances of injury. Blood vessel formation from preexisting blood vessel is a complex process known as angiogenesis. This process involves the interactions between various growth factors, the extracellular matrix (ECM), and several types of cells such as endothelial cells (ECs) and support cells.[125] Blood vessels are able to form via EC activities including attachment, proliferation, migration, and tube formation. Many of these processes are driven by growth factors. There are numerous growth factors that help regulate the cellular activities of endothelial cells including vascular endothelial growth factor (VEGF),[49] basic fibroblast growth factor (bFGF),[126] and platelet-derived growth factor (PDGF).[25] All of these growth factors are used in clinically available therapeutics, with VEGF being most important Though these pro-angiogenic

therapies show some efficacy in treating surface wounds, they possess some disadvantages, such as short half-life, slow diffusion, extremely high cost, and high risk of immune response due to extraction from animals or overloading.[127-128]

In addition to large growth factors, small peptide sequences containing the cell-binding motif of a native growth factor can be used as epitopes providing the desired innate bioactive responses. Several small peptide sequences that promote endothelial cell activity include Arg-Gly-Asp (RGD),[64] Ser-Val-Val-Thy-Gly-Leu-Arg (SVVGLYR),[83] Tyr-Ile-Gly-Ser-Arg (YIGSR),[65-66] and Ile-Lys-Val-Ala-Val (IKVAV).[67] The limitations of short peptide sequences derived from proteins include undesired clearance rates, poor metabolic stability, overloading, and possible immune responses.[84] Incorporating protein fragments in to self-assembling biomaterials can provide a high surface density of epitopes[13], increase metabolic stability, and reduce clearance rates. As a result, bioactive self-assembling peptides can provide a low-cost alternative for functional mimicry of large proteins with ease of modification.

Peptide amphiphiles (PAs) have been extensively studied as biomaterials for biotechnology and regenerative medicine. PAs, also known as lipidated peptides (LPs), are self-assembling peptides that form nanofibers.[114] This type of LP consists of a peptide sequence appended to a single alkyl tail. In addition to the alkyl tail, three structural regions or peptide components are typical. Region 1 is a short peptide sequence with high β-sheet propensity. Region 2 contains charged amino acids to enhance water solubility and for the design of pH and salt-responsive nanostructures and networks. The self-assembly of these LPs occurs when the strong electrostatic repulsion is either neutralized or screened about the aa in region 2. The third region consists of a bioactive peptide, an epitope that promote cellular response by interacting with receptors on the surface of cell membranes.[114]

Osteopontin (OPN) is a protein found in several areas of the body such as teeth, kidney, brain, and bone just to name a few.[129] The peptide sequence GRGDSVVYGLR contains the two motifs that guide OPN to bind with a number of integrins (RGD and SVVYGLR). The SVVYGLR motif, which is generated by thrombin cleavage at Arg-168, binds to the integrins $\alpha_4\beta_1$, $\alpha_4\beta_7$, and $\alpha_9\beta_1$ of cell membranes.[130] The synthetic peptide SVVYGLR has been shown to induce EC activity *in vitro* and *in vivo*, specifically promoting tube formation, proliferation and migration.[10] Park and associates constructed a SVVYGLR conjugated gelatin-poly(ethylene glycol)-tyramine hydrogel that enhanced endothelial cell activity and neo-vascularization.[131]

In this study, SVVYGLR (**SVV**) was attached to the C_{16}-$V_2A_2E_4$ self-assembling peptide motif with a GGG linker (C_{16} = palmitic acid). The LPs were investigated as bioactive injectable hydrogels to enhance EC activity and stimulate tube formation. The control peptide C_{16}-$V_2A_2E_2$ (**E_2**) was used as a diluent LP to vary the epitope loading.

2.2 Experimental Section

2.2.1 Materials

Rink Amide MBHA resin and Fmoc-protected amino acids were purchased from ChemPep, Inc. Palmitic acid (98%) was purchased from Acros organics. All other solvents and reagents were ACS reagent grade and were purchased from commercial sources and used as received.

2.2.2 Synthesis of all LPs

Rink amide MBHA resin (100-200 mesh; 0.48 mmol/g) was weighed into a reaction vessel. The resin was allowed to swell in dichloromethane (DCM) (10 mL) for 20 min prior to loading the first amino acid. A deprotection solution of 2% piperidine and 2% DBU in *N*,*N*-dimethylformamide (DMF) was used to remove the N-terminal Fmoc group. A portion of this solution (10 mL) was added to the reaction vessel, and the reaction mixture was agitated for 5 min. The solution was removed and this step was repeated once more. The resin was then washed with DCM (3 x 5 mL) and DMF (3 x 5 mL). A coupling solution of protected amino acid (4 equiv), *N*,*N*,*N*,*N*-tetramethyl-*O*-(1H-benzotriazol-1-yl)uranium hexafluorophosphate (HBTU) (3.9 equiv), and *N*,*N*-diisopropylethylamine (DIEA) (6 equiv) dissolved in 15 mL of DMF was added to the reaction vessel containing the resin, and the suspension was agitated for 2 h allowing for amide bond formation. The solution was drained and the resin was washed with DCM (3 x 5 mL) and DMF (3 x 5 mL). This procedure was repeated for each coupling step. After deprotection of the last amino acid (Val), C_{16} (4 equiv) was added using 1:1 DCM:DMF as the solvent to prepare the coupling solution. Once palmitic acid successfully coupled to the peptide, the LP was cleaved from the resin by treatment with trifluoroacetic acid (TFA)/ triisopropylsilane (TIPS)/H_2O (95/2.5/2.5) for 2 h under constant agitation. The cleavage solution containing the peptide was drained into a 250-mL round bottom flask, and the resin was washed with DCM (2 x 10 mL). The combined cleavage solution and washes were concentrated to 2 mL via rotary evaporation, and diethyl ether was added to precipitate out the peptide. The crude peptide was recovered via vacuum filtration, allowed to dry, and stored at 4 ˚C until HPLC purification. To dissolve the peptide after cleavage, 0.1% NH_4OH in milliQ water was added and

concentrated NH_4OH was added dropwise to adjust the pH to 8. The solution was passed through a 0.22 mm filter prior to HPLC purification.

2.2.3 Peptide Purification

Purification by preparative-scale reverse phase-high performance liquid chromatography (RP-HPLC) was carried out on an Agilent Technologies 1260 Infinity HPLC system, eluting with a gradient of 2% ACN to 100% ACN in milliQ H_2O using an Agilent PLRP-S column (100Å particle size, 25 x 150 mm) and monitoring at 220 nm. NH_4OH (0.1%) was added to both mobile phases during the purification of all peptides. Fractions were analyzed by mass spectrometry (Advion Expression Compact Mass Spectrometer), and product-containing fractions were combined, rotovapped to remove ACN, and lyophilized (LabConco).

2.2.4 Transmission Electronic Microscopy (TEM)

TEM samples were drop cast from 0.1 wt. % solutions of peptide in milliQ H_2O onto carbon-coated copper 300 mesh TEM grids (Electron Microscopy Sciences). Samples were then stained with a 2% solution of uranyl acetate in water. Images were taken on a Philips EM420 TEM with a slow scan CCD camera.

2.2.5 Viability and Cytotoxicity

To assess the cell viability and cytotoxicity activity in a single assay, ApoTox-Glo™ Triplex Assay was conducted. ECs were seeded in a 96-well plate at 15,000 cell/well in media. The appropriate solutions—media with $CaCl_2$ only, **E_2**, and 1:9 **SVV**:**E_2** were added to the well for a final volume of 100 μL. Cells were exposed to the treatments for 24 h, 48 h, and 72 h. A stock solution (20 μL), of Viability/Cytotoxicity Reagent containing both GF-AFC and bis-AAF-R110 substrates, was added each wells. The solution was mixed by orbital shaking (500 rpm for 1 min) and plates were incubated for 30 min at 37 °C. The fluorescence measurements for viability and cytotoxicity were conducted at $400_{Ex}/505_{Em}$ and $485_{Ex}/520_{Em}$, respectively.

2.2.6 Endothelial Tube Assay

Tube formation is an *in vitro* assay that recapitulates endothelial organization and several stages of angiogenesis. Basic procedures were used to determine the potential of **SVV** to promott tube formation *in vitro*. Hydrogels were prepared in 96 well plates with 25 μL 1:9 **SVV:E_2** or **E_2** followed by the addition of 5 μL of $CaCl_2$. After 10 min (allotted for gel stabilization), 15,000 cells were added to each coated well for a total volume of 100 μL. Plates were incubated for 8 h, 12 h, 24 h, 48 h, 72 h, and 96 h at 37 °C in a 5:95% CO_2:air incubator. Tube structures were observed and imaged under an Olympus Inverted Microscope and analyzed using Infinity software.

2.3 Results and Discussions

We sought to synthesize hydrogels that mimic the morphology of the extracellular matrix to promote endothelial tube formation. The design of the LP containing SVVYGLR was informed by the structural design of PAs, which are studied in the Stupp lab.[132] As illustrated in Fig. 8, the LPs were constructed by appending a palmitic acid tail to a peptide sequence made up of three regions: the β-sheet region (V_2A_2), the hydrophilic region (E_4), and the epitope region (SVVYGLR). The LP containing only $C_{16}V_2A_2E_2$ (**E_2**) was also designed and used as a control LP. Mixtures of **SVV** and **E_2** LPs were also prepared by mixing different mass ratios of **SVV** and **E_2**, thus controlling the loading of the epitope in the hydrogel. All peptides were synthesized by Fmoc solid phase peptide synthesis and purified by RP-HPLC. Excluding TEM, all further studies were conducted through the collaboration with the group of Professor Michelle Theus in the Virginia-Maryland Regional College of Veterinary Medicine at Virginia Tech.

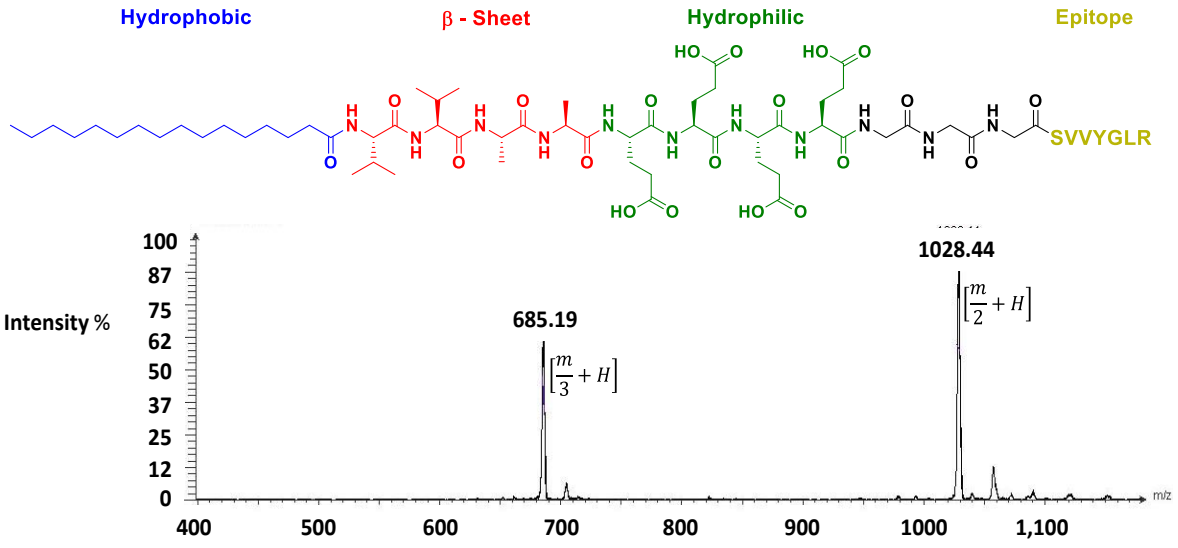

Figure 2.1: Chemical structure of the LP with the SVVYGLR epitope and EI mass spectrum.

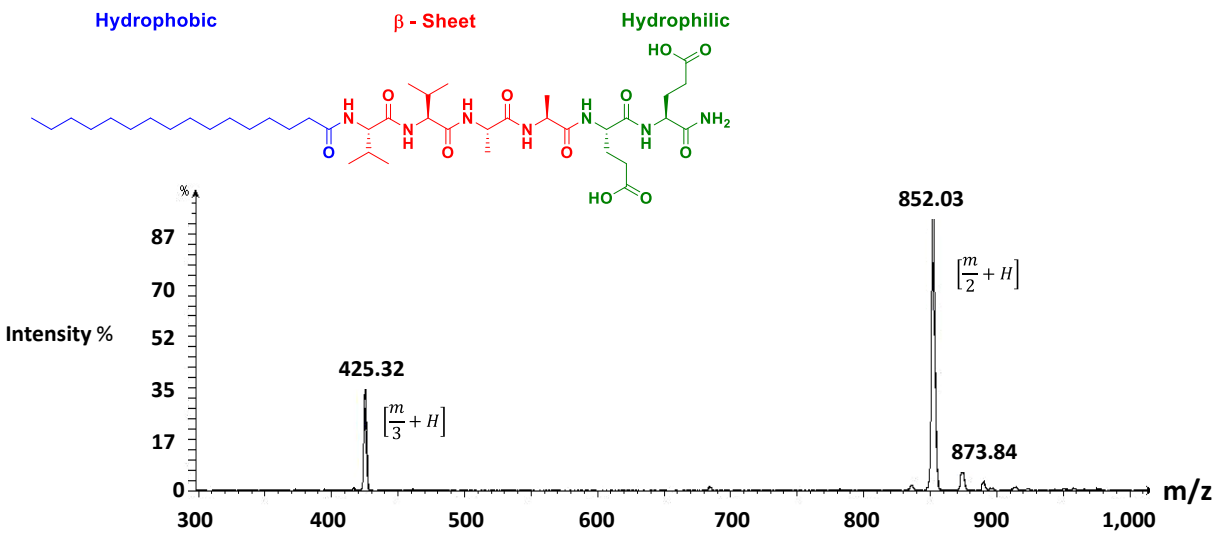

Figure 2.2: Chemical structure and EI mass spectrum of the control LP (without epitope).

Self-assembly of 1:9 **SVV:E**$_2$ (w/w) into a robust hydrogel was achieved by adding 1% w/v of the **SVV:**E$_2$ mixture to a 1-dram vial, followed by the addition of 20 µL of $CaCl_2$ (20 mM in H_2O) to induce charge screening (Fig. 10 inset). TEM images showed that the LP successfully self-assembled into nanofibers that were several microns in length with uniform diameter between 8 and 10 nm.

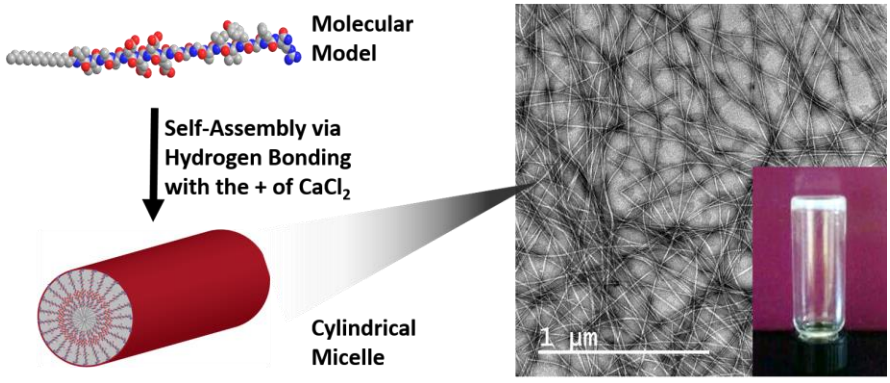

Figure 2.3: A schematic illustration showing the process of the LP self-assembly along with TEM of 1:9 (w/w) **SVV:E**$_2$. Inset demonstrates gelation of the material with $CaCl_2$.

The ApoTox-Glo™ Triplex Assay (Proemga corporation) measures three cell activities: viability, cytotoxicity, and apoptosis. This assay simultaneously measures both a cell viability marker, and a cytotoxicity marker. The live-cell protease activity is restricted to intact viable cells and is measured using a fluorogenic, cell-permeant, peptide substrate glycyl-phenylalanyl-amino-fluorocoumerin (GF-AFC). The substrate, restricted to intact viable cells, enters cells where it is cleaved by live-cell protease activity to generate a fluorescent signal proportional to the number of living cells. This live-cell protease becomes inactive upon loss of cell membrane integrity and leakage into the surrounding culture medium. A second substrate, bis-alanyl-alanyl phenylalanyl-rhodamine 110 (bis-AAF-R110), is used to measure cell death. This substrate interacst with dead cell protease, which is released from cells with damaged membranes. Because bis-AAF-R110 is not cell-permeant, essentially no signal from this substrate is generated by intact, viable cells. The different excitation and emission wavelengths of the fluorescent products, AFC and R110, allows for simultaneous detection.[133]

To evaluate both the viability and cytotoxicity of ECs in the presence of **SVV**, the ApoTox-Glo™ Triplex Assay was conducted. From these measurements, neither **E**$_2$ nor **1:9/SVV:E**$_2$ cell viability decreased relative to the control, as indicated by the decrease in the fluorescence of the coumarin dye (corresponding to live cells) after 48 h. The cytotoxicity of both LP was reasonably low (below 10%) for all intervals.

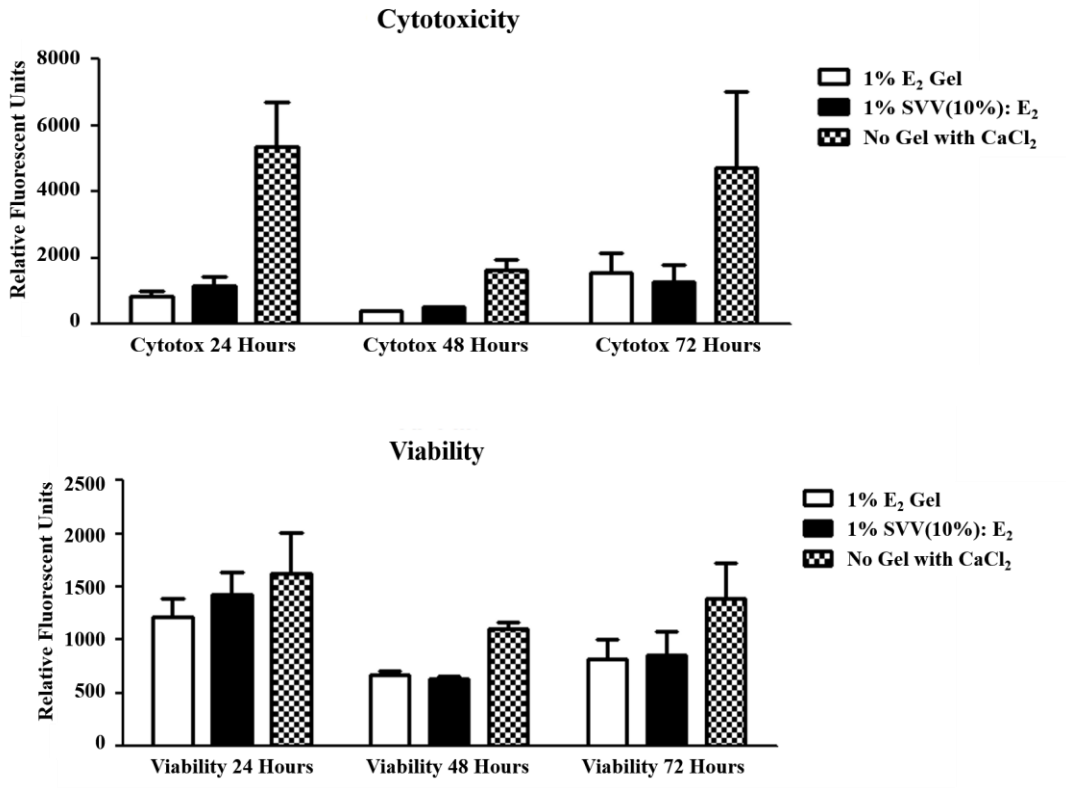

Figure 2.4: Cytotoxicity (*top*) and viability (*bottom*) of ECs with or without **SVV**

Differentiation of endothelial cells into a tube-like structure is an important step for angiogenesis. We investigated the effect of **1:9/SVV:E2** on the tube formation of ECs with different concentrations of $CaCl_2$. **1:9/SVV:E2** significantly induced the organization of ECs into tubular networks in $CaCl_2$ in a concentration dependent manner, as shown in Fig. 12. Variation of $CaCl_2$ concentrations affects the level of charge screening of the LP, thus varying the hydrogels' stiffness. **1:9/SVV:E2** with 0.1% $CaCl_2$ provided the highest level of EC tube formation after 24 h. Surprisingly, **E2** alone also induced tube formation. Comparing the two LPs, **1:9/SVV:E2** appeared to be more effective than **E2**, provide a more defined tubular network, with a greater number of cells present.

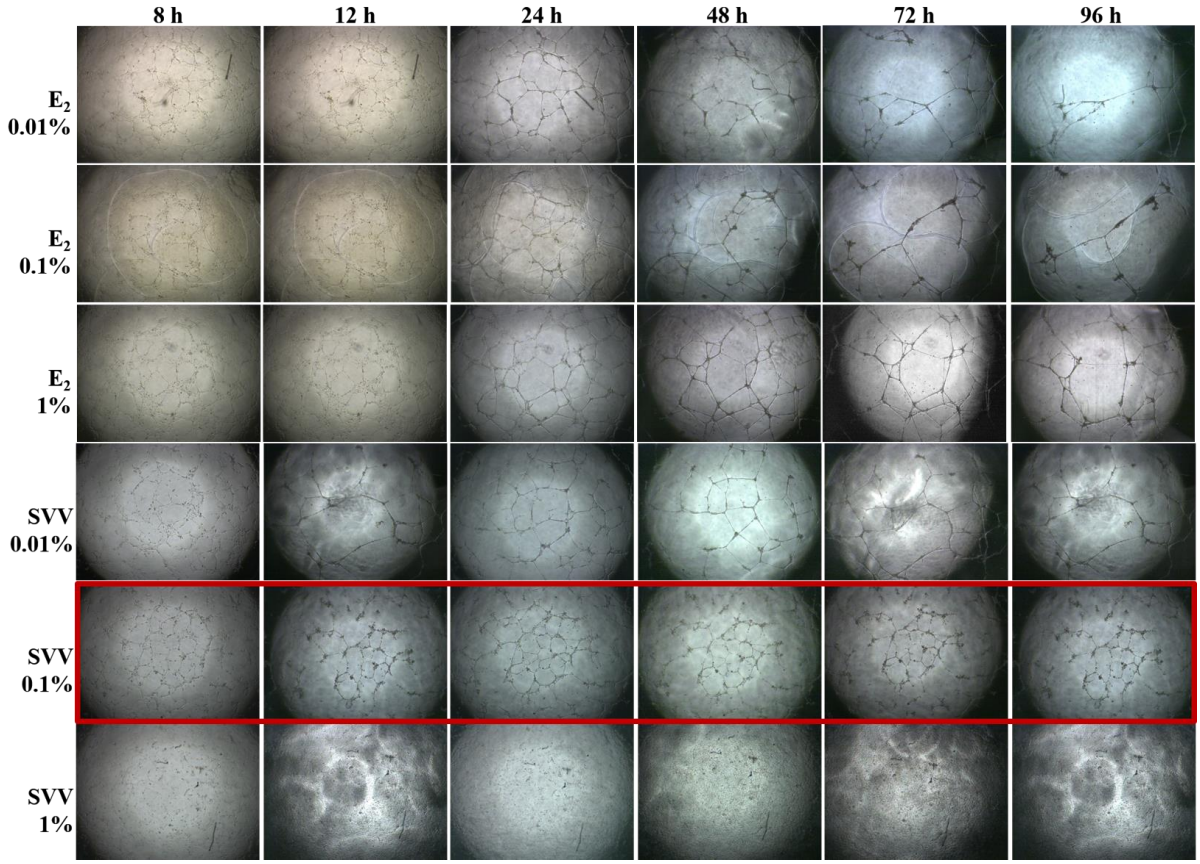

Figure 2.5: *In vitro* tube formation of MBECs employed by **1:9/SVV:E2** or **E2** hydrogels for 12 h, 24 h, 48, 72 h, and 96 h. Capillary tube structures were imaged with a digital camera attached to a microscope at 10x magnification.

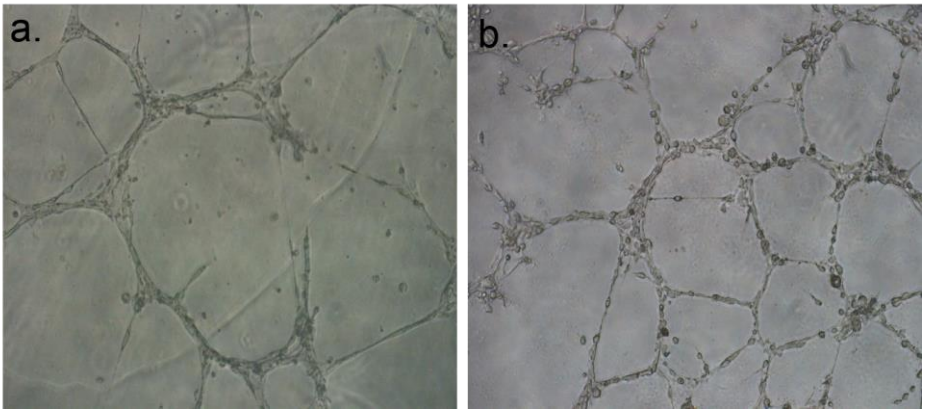

Figure 2.6: *In vitro* tube formation of MBECs employed by **E2** (a) and **1:9/SVV:E2** (b) for 24 h. Phase images of capillary tube structures were captured at 4x magnification. A more defined network is observed for the gel with the SVVYGLR sequence.

2.4 Conclusion

In conclusion, lipidated peptides with and without the SVVYGLR epitope were synthesized as a potential pro-angiogenic therapeutics. The two LPs were mixed at 1:9% ratios of **SVV** and **E_2** to control the loading of the epitope in the hydrogel. **1:9%/SVV:E_2** had low cytotoxicity and induced endothelial cell tube formation. However, the low viability effects of **SVV** on ECs may prevent it from being used as a pro-angiogenic therapeutic. This is an issue because without the improvement of cell growth survival, angiogenesis will not occur.

CHAPTER 3: HYDROGEN SULFIDE RELEASING PEPTIDE AMPHIPHILES

3.1 Introduction

Despite its reputation as a foul-smelling, toxic pollutant, hydrogen sulfide (H_2S) is a vital biological signaling gas (gasotransmitter) produced endogenously by various enzymes.[97, 134] Within the past few years, efforts devoted to studying the biological roles of H_2S and the enzymes that make it have expanded rapidly,[103-104, 135-136] along with related efforts to improve its detection *in vitro* and *in vivo*.[137-138] While many biological studies on H_2S are conducted using sulfide salts (NaHS and Na_2S), injections of aqueous sulfide solutions lead to a rapid surge of H_2S in the bloodstream followed by a rapid decline. To combat this uncontrolled delivery and more closely mimic the slow and sustained release of endogenous H_2S, our group and others have reported several classes of small molecules that release H_2S with controllable kinetics.[108, 110] However, despite this progress on small molecule H_2S donors, very few efforts have been made in the area of H_2S-releasing materials.[111-112]

In addition to H_2S, nitric oxide (NO) and carbon monoxide (CO) are also classified as gasotransmitters. The study of NO biology has benefitted greatly from NO-releasing materials, including polymers, gels, microparticles, and others.[139-140] The localized release provided by these materials allows for site-specific delivery of the gas, which minimizes the required dosage and off-target effects that can result from systemic NO administration. In fact, NO-releasing materials have been studied widely in preclinical animal models for preventing restenosis after balloon angioplasty.[42] Additionally, CO releasing materials have also been reported, although they have not yet reached the stage of animal models.[15, 141] In contrast, few H_2S-releasing materials have been prepared to deliberately release H_2S for potential use in therapy: two

polymeric H_2S donors[111-112] and one H_2S-releasing metal-organic framework.[142] To our knowledge, no reports exist to date describing gels that could potentially be used for localized H_2S release.

We recently reported the preparation of small molecule H_2S donors based on the *S*-aroylthiooxime (SATO) functional group, which release H_2S in response to thiol functionality.[110] These thiooxime compounds are prepared by reaction of an aroyl thiohydroxylamine (Ar-C(O)S-NH_2) (SATHA) with an aromatic aldehyde or ketone in the presence of a catalytic quantity of trifluoroacetic acid (TFA) and a drying agent (i.e. molecular sieves). H_2S release is triggered by thiols such as cysteine, and release rates can be tuned by changing substituents on the SATHA ring. As an extension of SATO chemistry, H_2S-releasing polymers show the versatility of this H_2S-releasing functional group.[112]

In this report, we describe the preparation of a self-assembling peptide designed to form gels that release H_2S. Self-assembling peptide-based materials include a wide range of peptide motifs that form one-dimensional nanostructures in aqueous solution. Gel formation in the range of 0.5-2 wt. % peptide can often be triggered by charge screening through pH changes or addition of salt; gelation then occurs through physical entanglement of the extended nanostructures. No chemical crosslinking is required, allowing for in situ gelation of the materials and shear-thinning behavior. These qualities, along with biocompatibility and biodegradability, make peptide-based gelators an attractive alternative to traditional polymeric hydrogels that require chemical crosslinking.

3.2 Experimental Section

3.2.1 Materials

Rink Amide MBHA resin and Fmoc-protected amino acids were purchased from ChemPep, Inc. 4-Formylbenzoic acid was purchased from Matrix Scientific. Dimethyl sulfoxide was purchased from Cambridge Isotope Laboratories, Inc. All other solvents and reagents were ACS reagent grade and were purchased from commercial sources and used as received. NMR spectra were recorded on a Varian Inova 400 MHz spectrometer. ^{1}H NMR chemical shifts are reported in ppm relative to internal solvent resonances. Yields refer to chromatographically and spectroscopically pure compounds. High-resolution mass spectra were taken in the Chemistry Analytical Facilities on an Agilent Technologies 6230 TOF LC/MS mass spectrometer.

3.2.2 Synthesis of FBA-IAVE$_3$

Rink amide MBHA resin (100-200 mesh; 0.48 mmol/g) was weighed into a reaction vessel. The resin was allowed to swell in dichloromethane (DCM) (10 mL) for 20 min prior to loading the first amino acid. A deprotection solution of 2% piperidine and 2% DBU in *N*,*N*-dimethylformamide (DMF) was used to remove the N-terminal Fmoc. 10 mL of this solution was added to the reaction vessel and the reaction mixture was agitated for 5 min. The solution was removed and this step was repeated once more. The resin was washed with DCM (3 x 5 mL) and DMF (3 x 5 mL). A coupling solution of amino acid (4 equiv), *N*,*N*,*N*,*N*-tetramethyl-*O*-(1H-benzotriazol-1-yl)uranium hexafluorophosphate (HBTU) (3.9 equiv), and *N*,*N*-diisopropylethylamine (DIEA) (0.6 mL, 6 equiv) dissolved in 15 mL of DMF was added to the reaction vessel containing the resin, and the suspension was agitated for 2 h. The solution was drained, and the resin was washed with DCM (3 x 5 mL) and DMF (3 x 5 mL). This procedure

was repeated for each coupling step. After deprotection of the last amino acid (Ile), the linker, 4-formylbenzoic acid (FBA) (4 equiv), was introduced using standard amino acid coupling procedures as described above. Once the linker was successfully coupled to the peptide, the peptide was cleaved from the resin by treatment with trifluoroacetic acid (TFA)/H_2O (97:3) for 2 h under constant agitation. The cleavage solution containing the peptide was drained into a 250-mL round bottom flask, and the resin was washed with DCM (2 x 10 mL). The combined cleavage solution and washes were concentrated to 2 mL via rotary evaporation, and then diethyl ether was added to precipitate out the peptide. The crude peptide was recovered via vacuum filtration, allowed to dry, stored at 4^{o}C until HPLC purification. To dissolve the peptide after cleavage, 0.1% NH_4OH in milliQ water was added and concentrated NH_4OH was added drop-wise to adjust the pH to 8. The solution was passed through a 0.22 mm filter prior to HPLC purification.

3.2.3 Synthesis of SATO-peptide

To a solution of FBA-$IAVE_3$ in DMSO (50 mg/mL) was added *S*--benzoylthiohydroxylamine (3 equiv). TFA (3 equiv) and activated 3 Å molecular sieves were added to the solution, as a catalyst and a drying agent, respectively. After 20 min, precipitation of the reaction mixture into dry DCM (20 mL) removed any excess SATHA and afforded crude peptide. The precipitate was vacuum filtered and placed under high vacuum to remove any residual DCM. Once dry, the product was stored in the freezer until purification. Just before purification, the crude product was taken up in milliQ water with 3 equiv K_2CO_3, which afforded

an aqueous solution at pH ~7. This solution was passed through a 0.22 mm filter prior to HPLC purification.

3.2.4 Purification

Purification by preparative-scale reverse phase-high performance liquid chromatography (RP-HPLC) was carried out on an Agilent Technologies 1260 Infinity HPLC system, eluting with a gradient of 2% ACN to 100% ACN in milliQ H_2O and using an Agilent PLRP-S column (100Å particle size, 25 x 150 mm) and monitoring at 220 nm. 0.1% NH_4OH was added to both mobile phases in the purification of **1**. MilliQ H_2O and ACN without any additives were used for the purification of **3**. Fractions were analyzed by mass spectrometry (Advion Expression Compact Mass Spectrometer), and product-containing fractions were combined, rotovapped to remove CH3CN, and lyophilized (LabConco). Peptide **1**: HRMS: m/z 820.3723 (820.3723 Calc m/z for [M+H+]), 843.3577 (843.3573 Calc for [M+Na+]), 858.3233 (858.3282 Calc for [M+K+]). Peptide **3**: HRMS: m/z 953.3713 (953.372 Calc for [M+H+]).

3.2.5 Circular Dichroism

Circular Dichroism measurements were carried out using a Jasco J-815 CD spectrometer at room temperature with a constant N_2 flow of 120 mL/min. The range of wavelengths employed was 400-190 nm (50 nm/min) with response time of 8 sec. The samples were measured in a 1 mm path length quartz cuvette. 200 µg of each sample was dissolved in milliQ H_2O (400 µL), and samples were briefly sonicated before analysis. MilliQ H_2O was used as a

blank. Between each measurement, the cuvette was rinsed with 3 cycles of water/ethanol/water. All measurements were conducted in triplicate.

3.2.6 Infrared Spectroscopy

FT-IR spectra were obtained on a Varian 670 FT-IR Spectrometer equipped with a diamond Specac Golden Gate attachment. All spectra were an average of 24 scans on powder form samples and were recorded from 4000 to 400 cm^{-1} with 4 cm^{-1} resolution. A background spectrum without sample was collected and subtracted from sample spectra.

3.2.7 Transmission Electron Microscopy

TEM samples were drop cast from 1 wt. % solutions of peptide in milliQ H_2O onto carbon-coated copper 300 mesh TEM grids (Electron Microscopy Sciences). Samples were then stained with a 2% solution of uranyl acetate in water. Images were taken on a Philips EM420 TEM with a slow scan CCD camera.

3.2.8 Rheology

All rheological studies were conducted on an AR-G2 rheometer. All time sweeps were performed at 1 Hz with 0.5% strain at rt using an ETC Disposable plate - 986680 (25 mm plate; 0.5 mm gap distance). 20 mM $CaCl_2$ (25 µL) was added to a 1 wt % solution of peptide in milliQ H_2O (250 µL), allowing it to gel on the rheometer. The reported storage moduli were taken from the time test at 60 min. Frequency sweeps were performed with a log ramp frequency of 0.01 – 100 Hz and a constant strain of 0.5%. Amplitude sweeps were performed with a constant frequency of 1 Hz and a log ramp strain of 0.1 – 100%. All rheological measurements were conducted in triplicate, and error bars represent the standard deviation.

3.2.9 Hydrogen Sulfide Release Experiments

A stock solution of 200 mM cysteine was prepared in PBS buffer (pH 7.4). A vial containing 3.98 mL of a 105-µM solution of **3** in PBS buffer. An H_2S-selective microelectrode (World Precision Instruments) was submerged into this solution, and the output current was allowed to equilibrate for several minutes under vigorous stirring. Once a stable current was observed, 20 µL of the cysteine solution was added to the vial for a final concentration of 1 mM. The current was monitored for approximately 2 h. No background subtraction was performed.

To analyze release of H_2S from peptide **3** in gel form, 40 µL of a 1 % wt. solution (~10 mM) of **3** was placed in a 1 dram vial. 20 mM aqueous $CaCl_2$ (4 µL) was added to induce gelation. After 5 min PBS buffer (3.94 mL) was added to the vial, and the microelectrode was submerged into the solution. After the output current stabilized, 20 µL of a 200 mM cysteine solution was added to the vial for a final cysteine concentration of 1 mM. The current was

monitored for approximately 10 h. A plot of H_2S concentration vs time was constructed using the calibration curve.

3.2.10 In vitro Studies

All cell studies were conducting using mouse brain endothelial cells (MBECs) which were maintained in a T-25 polystyrene culture flask with endothelial cell media (Cell Biologics) at 5% CO_2 and 37 ^{0}C. Subcultures were done with trypsin-EDTA solution. For all experiments presented cells between passages 7-10 were used.

Initially, cell viability assays were conducted using tetrazolium compounds including MTS and MTT, to determine cell proliferation capability. The MTT tetrazolium compound is biologically reduced by cells into a colored formazan as crystalline precipitate. The insoluble crystals must be dissolved, usually with DMSO, before measuring the absorbance at 570 nm. This reduction occurs by NADPH or NADH produced by dehydrogenase enzymes in metabolically active cells.[143]

The MTS assay is also comprised of a tetrazolium compound, 3-(4,5-dimethylthiazol-2-yl)-5-(3-carboxymethoxyphenyl)-2-(4-sulfophenyl)-2H-tetrazolium (MTS). This compound is usually prepared in solution with an electron-coupling reagent to enhance the stability of the MTS solution. The formazan product of MTS reduction is soluble in tissue culture media, resulting in the elimination of the intermittent steps that are required in MTT assay. This reduction reaction only takes place when mitochondrial reductase enzymes are active; therefore, the absorbance measured at 490 nm is directly proportional to the number of living cells in

culture.[144] Although these assays maybe useful for standard cytotoxicity assays, the tetrazolium functional groups are not stable in the presence of cysteine at 1 mM.

Due to the suspected tetrazolium interaction with cysteine, the cytotoxicity measurements were obtained by live/dead assay (Calcein AM and ethidium homodimer) on C57BL/6 mouse primary brain microvascular endothelial cells.

The LIVE/DEAD® Viability/Cytotoxicity assay provides two probes that measure cell viability—intracellular esterase activity and plasma membrane integrity, allowing for simultaneous determination of live and dead cells, respectively. Calcein AM and ethidium homodimer (EthD-1) are the dyes that can detect cell viability or cytotoxicity by several fluorescence detection systems.

Live cells are detected by measuring the presence of ubiquitous intracellular esterase activity, determined by the enzymatic conversion of cell-permeant Calcein AM to fluorescent Calcein. Calcein is a polyanionic dye that produces an intense uniform green fluorescence in live cells (ex/em ~495 nm/~515 nm). Upon the binding to nucleic acids that are accessible from damaged cell membranes, EthD-1 undergoes a 40-fold enhancement of fluorescence in dead cells (ex/em ~495 nm/~635 nm). EthD-1 is excluded by the intact plasma membrane of live cells.

Each experiment was repeated three times with n=5 for each run, and error bars reflect the standard deviation. Cells were passaged using standard cell culture procedures. Before plating, cells were detached with trypsin and centrifuged (3000 rpm for 5 min). The supernatant was removed, and the cells were resuspended in 1 mL complete endothelial cell media (Cell Biologics), and counted. Cells were plated in a 96-well plate at a concentration of 10,000 cells/well in a 96-well plate and incubated overnight (37 °C, 5.0% CO2). PA **3** was dissolved in PBS at 80 μM. The peptide solution was diluted with basal media or basal media containing 1

mM cys to obtain peptide concentrations of 80 μM, 60 μM, 40 μM, 20 μM, and 2 μM. Control wells contained basal media or basal media with 1 mM Cys. After incubating for 24 h (37 °C, 5.0% CO_2), the media was replaced with live/dead solution (made per the manufacturer's instructions), and the plate was left to incubate for 15 min. Cells were imaged and counted on a Nikon Eclipse Ti-U inverted fluorescent microscope.

Cytotoxicity measurements for the peptide in gel form were carried out using the same live/dead stains as above. Using the same passaging and plating protocol as above, cells were seeded at 20,000 cell/well in a 48-well plate and incubated overnight (37 °C, 5.0% CO_2). Before gels were added, the media was removed and replaced with basal media or basal media with Cys (1 mM). Peptide gels were prepared in Slide-A-Lyzer dialysis cups (2000 MWCO, Thermo Scientific) at 1% w/v by adding 30 μL PA **3** to the cup followed by the addition of 3 μL of 2 mM $CaCl_2$. After 10 min, the cups were placed in wells, and 50 μL of basal media (with or without Cys) was added to cover the gel. After incubating for 24 h (37 °C, 5.0% CO_2), the cups and media were removed from the wells, and live/dead solution was added. The plate was left to incubate for an additional 15 min before imaging as above.

3.2.11 Fluorescence Probe studies of H_2S uptake in vitro

A selective turn-on fluorescent probe was used to confirm H_2S uptake *in vitro*.[138] An amino-naphthalimide fluorescent compound containing an azide group, was chosen due to its ease of synthesis and large Stokes shift. Pluth and associates developed a fluorogenic amine containing a nitro or azide group that once reduced by H_2S, will generate fluorescence.[138] Using this platform, we synthesized a third amino-naphthalimide fluorescent probe, in which 2-

methoxyethyl-amine was replaced with 2-aminoethan-1-ol. This new probe was named Hydrosulfide Naphthalimide-3 (HSN-3) and has λ_{Em} = 542 nm, which is in the range of the other probes developed by Pluth.

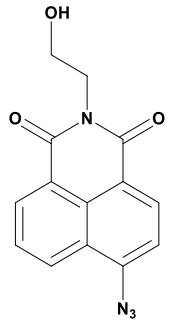

Figure 3.1: Chemical structure of HSN-3

Detection of H_2S uptake *in vitro* was analyzed using a turn-on fluorescent probe selective for H_2S.[138] C57BL/6 cells were cultured at 5,000 cells/well in 0.1 mL of complete media and incubated for 48 h. After aspiration of the media, the cells were washed with PBS (1X) and incubated with the probe (**HSN3**) (5 μM) in PBS. After 20 min, **3** in PBS at 100 μM, with (+) or without cysteine (–) was added to the cells and incubated for an addition 20 min. Solutions were removed and the cells were washed once more and bathed in PBS for fluorescent imaging.

3.3 Results and Discussions

One class of self-assembling peptides is the peptide amphiphiles (PAs).[114] PAs are comprised of short β-sheet oligopeptides appended to a hydrophobic alkyl tail. The peptide sequences are typically designed to self-assemble in water into extended cylindrical micelles or nanofibers.[145] Self-assembly of PAs can also be achieved by incorporating an aromatic moiety. The H_2S-releasing peptide in this report was designed to take advantage of the inherent

hydrophobicity of the SATO motif to achieve amphiphilicity as well as exploit the hydrogen bonding of a short β-sheet-forming oligopeptide (Figure 15). We envisioned that a SATO-functionalized PA could be utilized to prepare a hydrogel with H_2S-releasing capability. Toward this end, the peptide $IAVE_3$ was synthesized under standard solid phase conditions using Fmoc chemistry. The β-sheet region was designed based on the propensity of certain residues to self-pair.[119] It has been shown that Ala, Ile, and Val exhibit the highest tendency to self-pair; therefore, we incorporated these amino acids into the peptide sequence. On resin, the addition of formylbenzoic acid was conducted under the same conditions as typical amino acid coupling, giving the modified peptide FBA-$IAVE_3$ (**1**). Following cleavage and purification via RP-HPLC, the modified peptide was allowed to react with *S*-aroylthiohydroxylamine (**2**) in the presence of 3 equiv of TFA, employing molecular sieves as a drying agent (Figure 15). An excess of acid catalyst was necessary due to neutralization of the acid catalyst by the carboxylate residues in PA **1**.

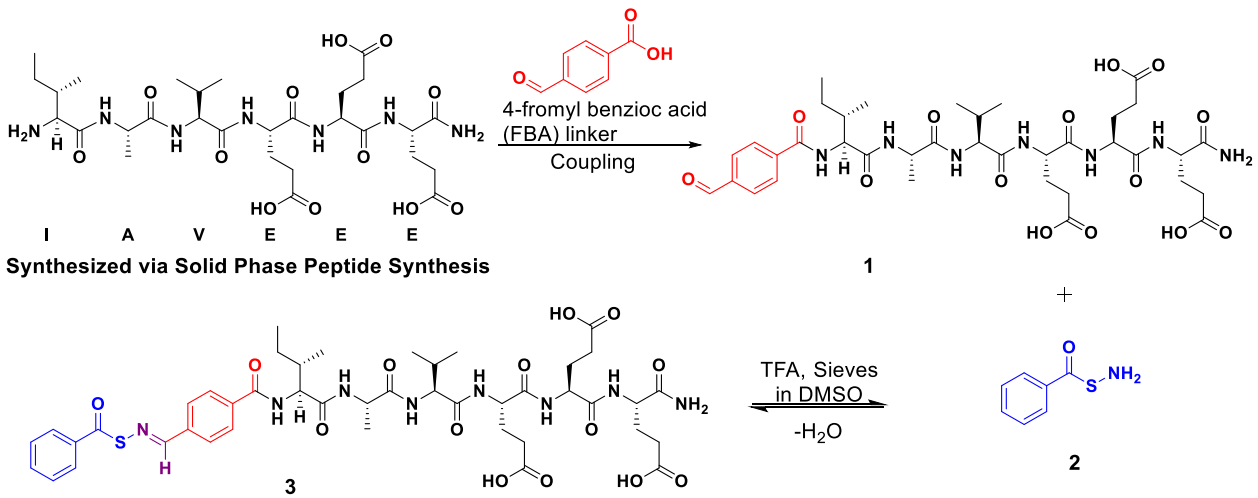

Figure 3.2: Synthesis of the SATO-peptide.

Deuterated dimethyl sulfoxide (DMSO-d_6) was chosen as the solvent, and the conversion to thiooxime was monitored by ^{1}H NMR spectroscopy by comparing the integration of the aldehyde resonance of peptide **1** at 10.05 ppm (Figure 16) to the thiooxime proton of peptide **3** at 9.05 ppm (Figure 17). Full conversion was observed after 20 min, evident by the complete disappearance of the aldehyde resonance. Electrospray ionization mass spectrometry (ESI-MS) further corroborated the success of SATO formation. Precipitation of the reaction mixture into DCM afforded PA **3**, which was further purified via RP-HPLC.

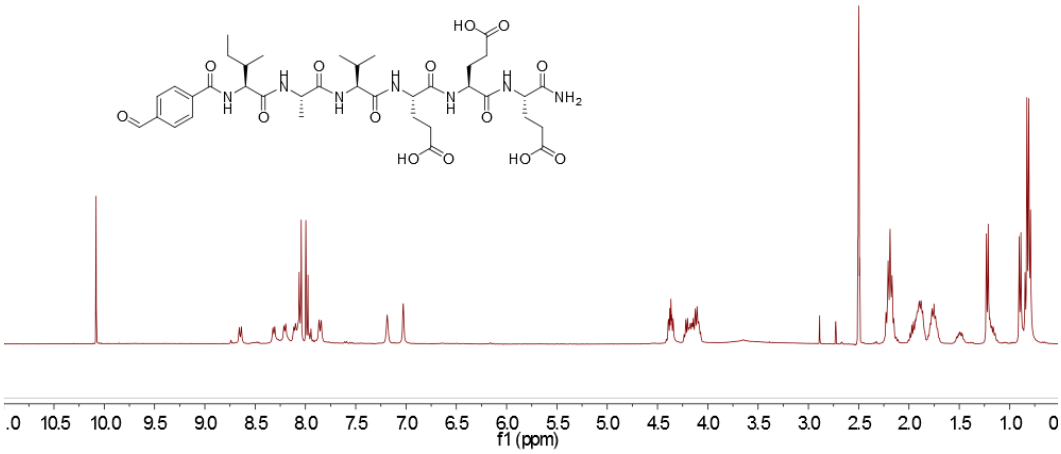

Figure 3.3: ^{1}H NMR spectrum of **1.**

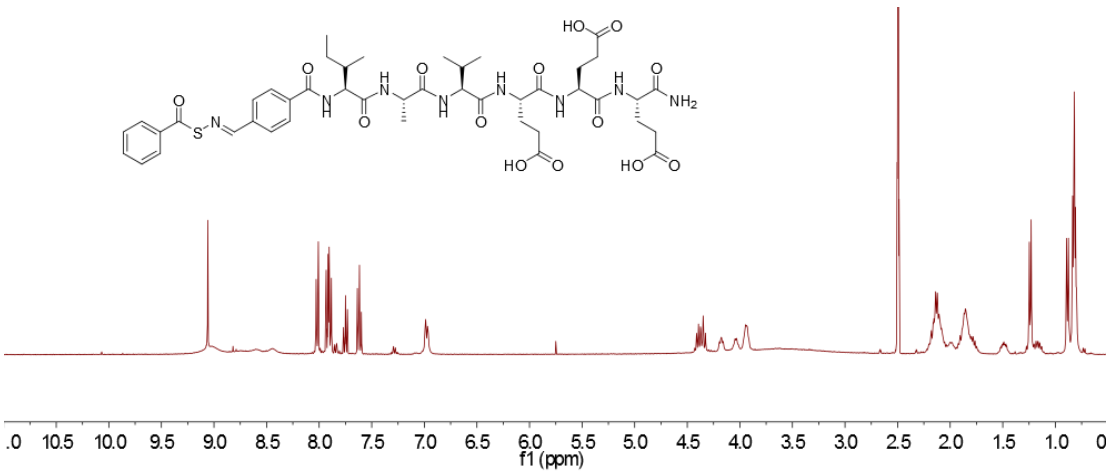

Figure 3.4: ^{1}H NMR spectrum of **3.**

Transmission electron microscopy (TEM) was used to characterize the morphology of the self-assembled architecture of PA **3**. To prepare samples for analysis, **3** was dissolved in H_2O at 1 w/v% and TEM grids were drop coated with this solution and then negatively stained with uranyl acetate. Because of the structural similarity of PA **3** to traditional self-assembling PAs, it was expected to adopt a nanofiber morphology in solution. Figure 18a shows the TEM of PA **3,** having a dominant presence of long, one-dimensional nanofibers with an average diameter of 10 nm. Additionally, we hypothesized that the reduced hydrophobic volume of PA **1** relative to PA **3** would result in the self-assembly of PA **1** into relatively shorter nanofibers or spheres.

We were interested to observe whether the nanofibers could for a self-supporting gel under charge-screening conditions. The addition a of divalent salt such as $CaCl_2$ initiates the formation ionic bridges between the negatively charged glutamic acid residues, reducing the Debye screening length of the molecules and allowing closer packing of the peptide strands.[146] Solutions of PAs **1** and **3** in milliQ H_2O at 1 wt.% were prepared, and 20 mM of $CaCl_2$ was added to each to screen charges and promote aggregation. As shown in Figure 18b, PA **3** formed a robust hydrogel (images 1-2), while PA **1** did not. The fact that PA **1** does not form a hydrogel may be useful in vivo to ensure degradation of the gel into peptides that can be easily metabolized. This is an important property for biocompatible and biodegradable therapeutics.

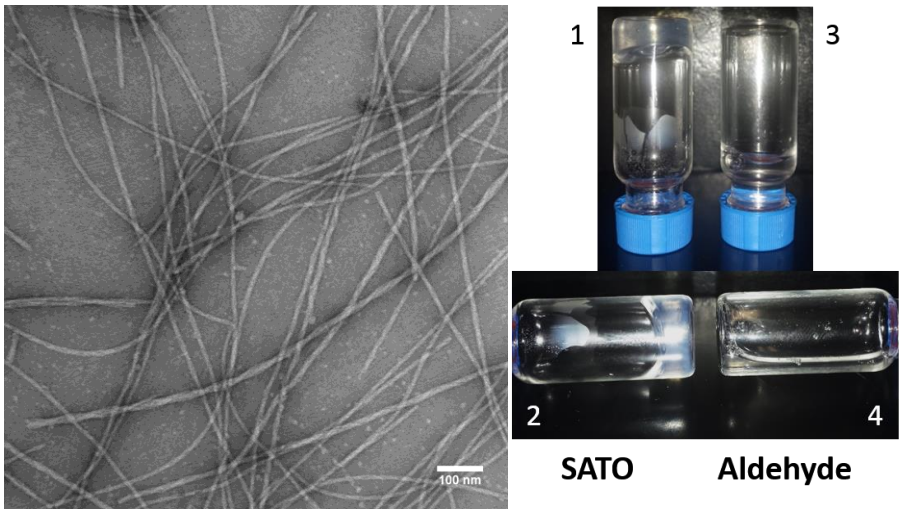

Figure 3.5: (a) Negative Stained TEM of **3**; (b) Visual image of **3** (1-2) & **1** (3-4) with $CaCl_2$.

The viscoelastic properties of the self-assembled peptide hydrogels prepared from PAs **1** and **3** were characterized by rheology. A material is considered a gel when its storage modulus *(G')* is considerably greater than its loss modulus (*G")*. To study the rheological profile of PA **3** in gel phase, the PA was dissolved in H_2O at 10 mg/mL and 25 uL of a 20 mM solution of $CaCl_2$ was added.

The rheological profiles of PAs **1** and **3** are shown in Figures 19 and 20. Prior to the frequency sweep, a time sweep was performed to allow for maximum gelation. As shown in Fig. 19a, the *G'* for PA **3** increased as a function of time and quickly plateaued at ~300 Pa. Under these same conditions the *G'* for PA **1** remained leveled at 1 Pa, indicating there was no occurrence of gel formation. As a result, no further rheological studies were performed. These findings coincide with the fact that gel formation was not observed in the vial inversion tests, likely due to the short hydrophobic segment of PA **1**. During the frequency sweep for peptide PA **3**, *G'* and *G"* remained steady independent of frequency, and no crossover of the two was observed, even up to 100 Hz.

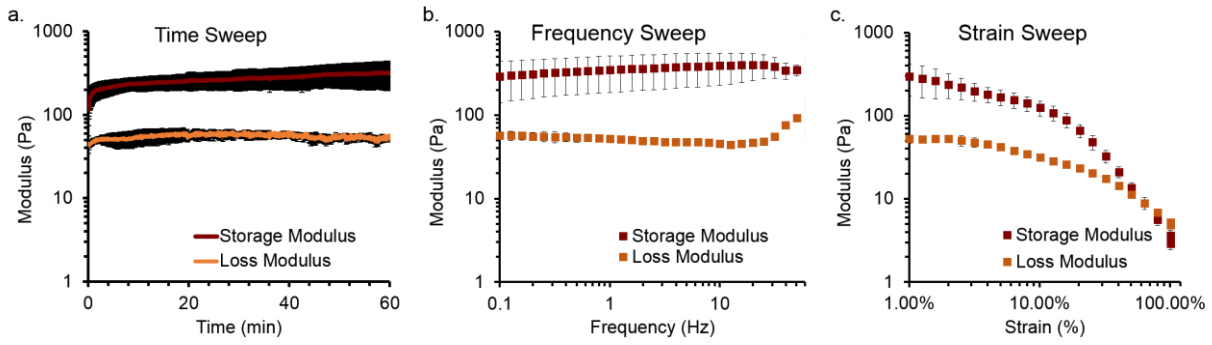

Figure 3.6: Rheological measurements of **3**; (a) time sweep, (b) frequency sweep, (c) strain sweep.

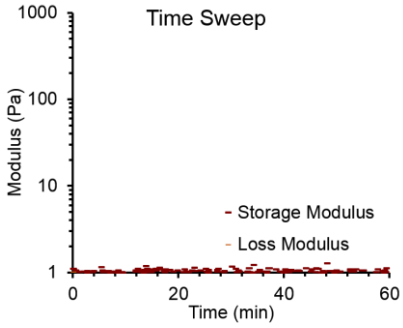

Figure 3.7: Rheology time sweep measurements of peptide **1**.

Circular dichroism is a method used to examine secondary structures of proteins and peptides. CD measures the absorption of left- and right- circularly polarized light. Upon the absorption of light, electrons transition into their excited state inducing a dipole moment in the molecule. These induced dipole moments will then interact with one another. The amide groups in proteins possess well characterized low energy transitions π-π* and n-π*, whose locations and intensities indicate secondary structural features of the peptide sequence.[147] Prolific hydrogen bonding localized in the β-sheet region of the peptide sequence of PAs typically results in the presence of a negative n-π* transition between 216-218 nm, and a positive π-π* transition at ~198 nm in the CD spectrum. α-helical proteins have a negative n-π* transition at 222 nm and

208 nm and a positive π-π* transition at 193 nm. Proteins with disordered secondary structures have a negative band with great magnitude at ~200 nm.[148]

The CD spectra of PAs **1** and **3** had no appearance of a secondary β-sheets but rather a disordered "random coil" secondary structure with a negative π-π* transition at 199 nm, Figure 21.

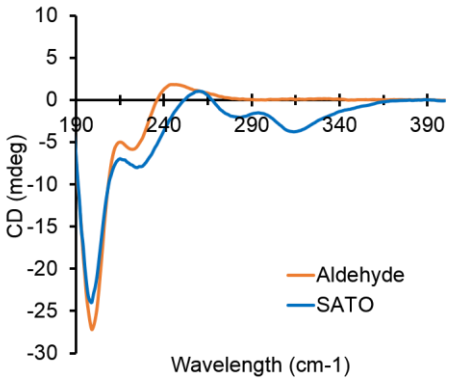

Figure 3.8: Circular dichroism trace of PAs **1** (aldehyde) and **3** (SATO)

Infrared spectroscopy (IR) is used to detect the vibrational processes in a molecule. Since each vibrational mode has its own resonant frequency, one can determine the functional groups present in a molecule. The amide I band (1600–1700 cm^{-1}) in proteins is the most studied vibration because its bands are sensitive to the type and amount of secondary structures. Also the amide I band is not strongly influenced by side chains.[149-150] β-sheets have a strong absorption band near 1630-1640 cm^{-1} and a weaker band at high frequencies (~1680 cm^{-1}). The band for α-helices and random coils are located at 1640-1660 and 1640-1650 cm^{-1}, respectively.

The vibrational processes of PA **1** and **3** were analyzed via FTIR. As shown in Figure 22, there was a strong peak at 908 cm^{-1} present in the IR spectrum of PA **3** but not in PA **1**. This band represents the N–S stretch indicative of the SATO functionality. The IR spectrum of PAs **1** and **3** as a powder both exhibited strong amide I bands ($\nu_{C=O}$) at ~1625 cm^{-1}, indicative of a β-

sheet structure. The IR spectrum of PA **3** in the gel phase also displayed the presence of a β-sheet structure with a band at 1619 cm^{-1} as well as a increase frequency peak at 1673 cm^{-1}. Unfortunately, the IR data was not in agreement with the CD data, indicating that the peptides are self-assembling not as a result of β-sheet hydrogen bonding or π-π stacking, but simply because of the peptides amphiphilic nature.

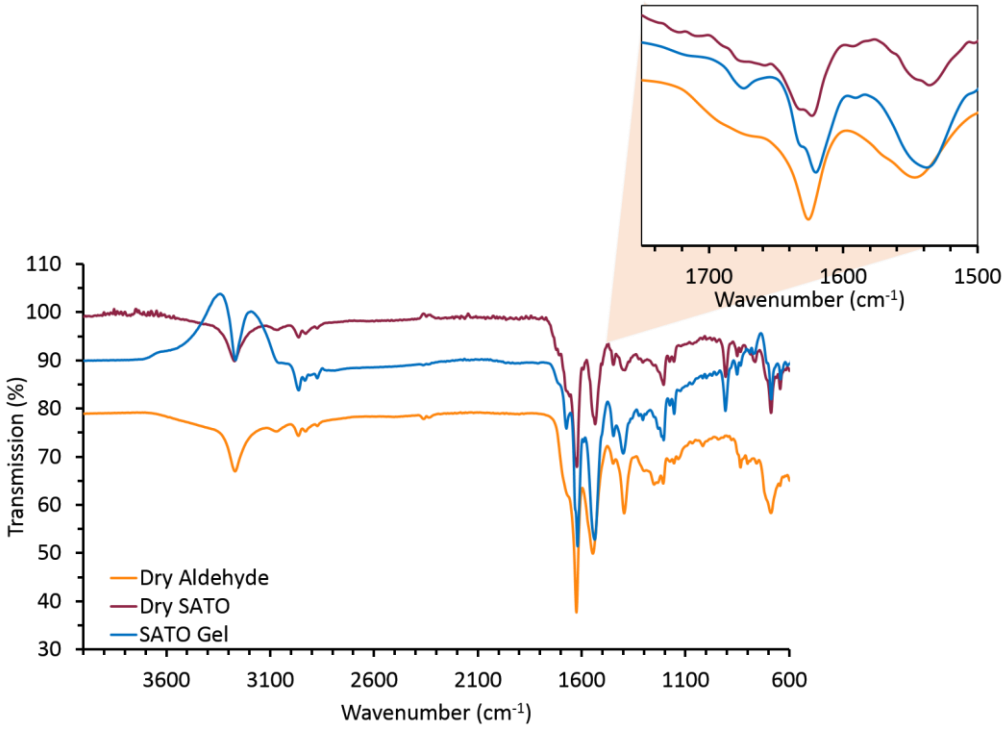

Figure 3.9: IR of aldehyde-peptide powder, SATO-peptide powder, and SATO-peptide hydrogel with the amide I band ($\nu_{C=O}$) range (insert), exhibited a band at ~1625 cm^{-1}, indicative of a β-sheet structure.

The rate of H_2S release from PA **3** was assayed using an H_2S-selective microelectrode. This method allows for real-time monitoring of the concentration of H_2S in solution, giving an indirect measurement of the relative rate of the H_2S-releasing reaction. To evaluate the H_2S release profile of PA **3** in solution, a PBS solution containing 100 μM of PA **3** was treated with 1

mM cysteine and the resulting concentration of H_2S was measured as a function of time. As illustrated in Figure 23, PA **3** in solution had a rapid release of H_2S, reaching 11.7 μM after 83 min. The concentration of H_2S began to decrease minutes after reaching the maximum concentration. The observed H_2S release profile of PA **3** in solution is similar to those of the small molecule thiooxime donors previously investigated.[110]

When **3** is in the gel phase, Cys diffusion into the hydrophobic core of the nanofibers is likely limited. Thus, we expected a slower release of H_2S in gel form than in soluble form. To determine effect of gelation of PA **3** on its H_2S release profile, PA **3** in gel phase was treated with Cys, and the evolution of H_2S was monitored with a H_2S-selective electrode. As shown in Figure 23, the rate of H_2S release was substantially slower in the gel phase than the H_2S release of PA **3** in solution. Interestingly, a clear peaking time was not identified; instead there was a constant release over the next 50 min.

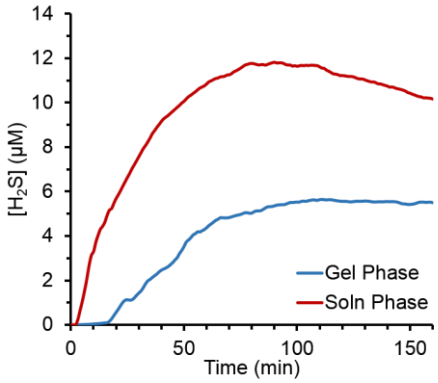

Figure 3.10: Representative H_2S release curve of PA **3** in solution and gel phase using a H_2S sensitive microelectrode.

The live/dead fluorescence assay was used to assess if PA **3** exhibits any cytotoxicity in C57BL/6 primary mouse brain microvascular endothelial cells). Cytotoxicity of PA **3** in solution

was first analyzed at different concentrations, with and without Cys. After 24 h of treatment, Live/Dead stain was added and the cell were imaged.

Next, the cytotoxicity of PA **3** in the gel phase at 0.1 mM with and without cysteine was analyzed (Figure 24b). There was no toxic effects caused by PA **3** in the gel phase with and without cysteine. The decrease in viable cells has no significant differences and is due to random errors.

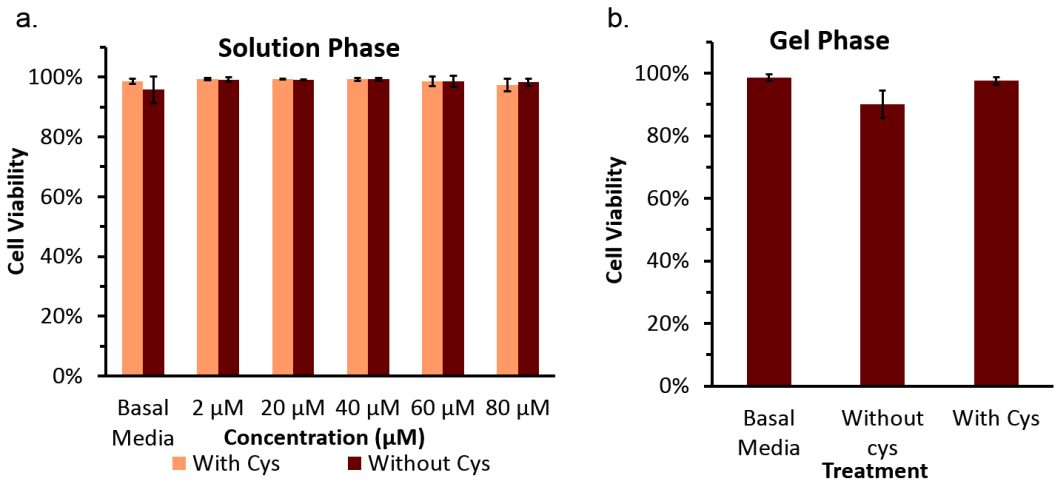

Figure 3.11: Cytotoxicity assays of PA **3** in sol (a) and in gel (b) phase.

H_2S is endogenously produced at concentrations ranging from 100s of nM level up to 10s of µM level. For delivery of exogenous H_2S, a report has shown a 2-fold increase in proliferation for human endothelial cells when exposed to 60 µM H_2S.[104] It has also been shown that H_2S is transported through cell membranes without any regulatory transports via a passive diffusion mechanism. Despite a significant dipole moment and large polarization, H_2S is solvated and permeates membranes like a hydrophobic solute.

Detection of H_2S release from PA **3** on C57BL/6 cells *in vitro* was analyzed using a turn-on fluorescent probe selective for H_2S (HSN3).[151] As shown in Figure 25, the addition PA **3** to the cells pre-incubated with HSN3 showed strong fluorescence, demonstrating that this H_2S-releasing peptide has the ability to successful delivery H_2S to ECs. To confirm the fluorescence was a result of the H_2S released from the peptide, several controls were performed: HSN3 only, HSN3 plus Cys, and HSN3 plus PA **3** without cys. Though fluorescence was observed when the cells were treated with Cys, the intensity was extremely low when compared to the cells treated with PA **3** in the presence of Cys. Weak fluorescence was observed for the group that included HSN3 and PA **3** without Cys, implying that sufficient thiol functionality exists in solution or within the cells themselves to trigger H_2S release.

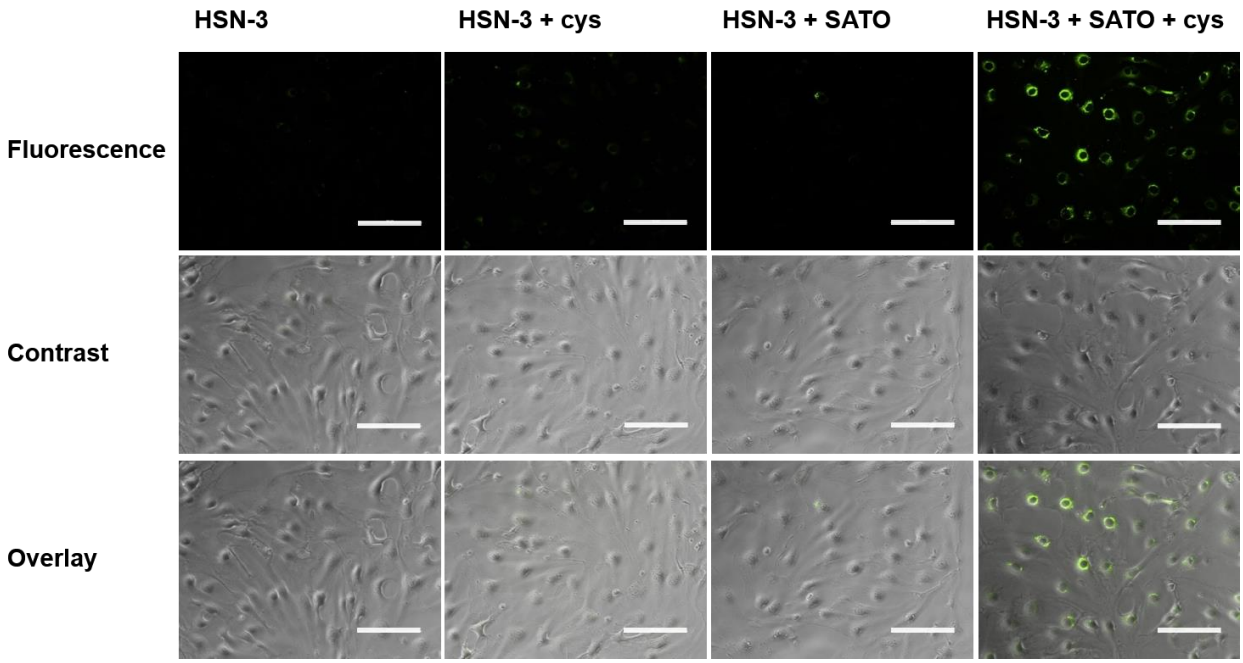

Figure 3.12: Fluorescence imaging of H_2S in ECs with HSN3, column 1, 2, and 3 show the fluorescence, fluorescence and contrast overlaid respectively.

3.4 Conclusions

In summary, an H_2S-releasing peptide containing the SATO functionality was synthesized. It was shown that the SATO-peptide self-assembles based on its amphiphilic nature in to a robust hydrogel possessing a nanofiber morphology. We demonstrated that the release of H_2S could be controlled by changing the state of the peptide, either in solution or in gel phase. Furthermore, live/dead assays showed that the SATO-peptide had no cytotoxic effects on endothelial cells. It was also demonstrated that the SATO-peptide can successfully deliver H_2S to ECs in the presence of a thiol.

CHAPTER 4. SUMMARY & FUTURE DIRECTIONS

4.1 Summary

Currently, no treatments have been shown to improve brain dysfunction after a people endures traumatic brain injury. Earlier strategies to improve brain function after TBI used a neurogenesis approach. However, it was later shown that adult neurogenesis occurs in the content of angiogenesis. From these findings, we focused on the preparation of self-assembling peptides for use as pro-angiogenic therapies. Our approach consisted of two biomaterials: The first system was designed using the traditional lipidated peptide structure containing the SVVYGLR epitope; the second system was designed as an H_2S-releasing peptide containing the SATO functionality.

The SVVYGLR-based material showed low cytotoxicity and induced endothelial cell tube formation. However, the **SVV** inability to proliferate ECs interjects any possibility of this materials use as an angiogenic therapeutic. This is an issue because without the improvement of cell growth and survival, angiogenesis will not occur.

It was shown that the SATO-peptide self-assembles based on its amphiphilic nature into a robust hydrogel possessing a nanofiber morphology. We demonstrated that the release of H_2S could be controlled by changing the state of the peptide, either in solution or in gel phase. Furthermore, the live/dead assays shown that the SATO-peptide had no cytotoxicity effects on endothelial cells. It was also demonstrated that the SATO-peptide can successfully deliver H_2S to ECs in the presence of a thiol trigger.

4.2 Recommended Future Work

In the first approach, the peptide amphiphiles containing the epitope SVVYGLR were designed with a traditional hydrophobic fatty acid tail. Palmitoylethanolamide (PEA), an endogenous fatty acid amide, is present in the brain and has anti-inflammatory, neuroprotective,[152] and antinociceptive[153] properties effective in mice. The main target of PEA is the receptor proliferator-activated receptor alpha (PPAR-α)[154], which regulates pain and inflammation.[155] It would be interesting to use this and other fatty acids that are present in the brain as hydrophobic tails. They may enhance the overall activity of the PA for TBI treatments.

In the second approach, peptide amphiphiles containing the SATO functionality were prepared as biomaterial with H_2S-releasing capability. It would be interesting to investigate tube formation of endothelial cells and *in vivo* studies employed by these H_2S-releasing peptides.

To further elucidate the self-assembled structure of the SATO-peptide, it is necessary to conduct further structural investigations such as:

1. Varying the concentration of the SATO-peptide during IR measurements.
2. Determining the CMC value of the peptide using the Nile red assay.
3. Analyzing the self-assembling process during pH and temperature changes.

As reported in the recent publication on the SATO functional groups, the release of H_2S from these molecules is dependent on the substitutions attached to the SATHA ring. The half-lives ranged from 8−82 min.[110] It would be interesting to modify the structural design of the SATO group to develop a range of controlled release rates of the SATO-peptide. The studies mentioned above could improve the properties of H_2S-releasing peptides, which will advance their potential as pro-angiogenic therapies.

REFERENCES

1. Folkman, J. *Nat Med* **1995,** *1* (1), 27-30.
2. Carmeliet, P. *Nature* **2005,** *438* (7070), 932-936.
3. Carmeliet, P. *Nat Med* **2003,** *9* (6), 653-660.
4. Wieman, T. J. *Am J Surg* **1998,** *176* (2, Supplement 1), 74S-79S.
5. Aviles, R. J.; Annex, B. H.; Lederman, R. J. *Br J Pharmacol* **2003,** *140* (4), 637-646.
6. Zaulyanov, L.; Kirsner, R. S. *Clin Interv Aging* **2007,** *2* (1), 93-98.
7. Mostow, E. N.; Haraway, G. D.; Dalsing, M.; Hodde, J. P.; King, D. *J Vasc Surg* **2005,** *41* (5), 837-843.
8. Morykwas, M. J.; Argenta, L. C.; Shelton-Brown, E. I.; McGuirt, W. *Ann Plast Surg* **1997,** *38* (6), 553-562.
9. Negative Pressure Wound Therapy Devices: Technology Assessment Report. October 2014. http://archive.ahrq.gov/research/findings/ta/negative-pressure-wound-therapy/index.html.
10. Egusa, H.; Kaneda, Y.; Akashi, Y.; Hamada, Y.; Matsumoto, T.; Saeki, M.; Thakor, D. K.; Tabata, Y.; Matsuura, N.; Yatani, H. *Biomaterials* **2009,** *30* (27), 4676-4686.
11. Jonker, A. M.; Löwik, D. W. P. M.; van Hest, J. C. M. *Chem Mater* **2012,** *24* (5), 759-773.
12. Wang, R. *Proc Natl Acad Sci* **2012,** *109* (23), 8801-8802.
13. Webber, M. J.; Kessler, J. A.; Stupp, S. I. *J Intern Med* **2010,** *267* (1), 71-88.
14. Fleming, S.; Ulijn, R. V. *Chem Soc Rev* **2014,** *43* (23), 8150-8177.
15. Matson, J. B.; Webber, M. J.; Tamboli, V. K.; Weber, B.; Stupp, S. I. *Soft Matter* **2012,** *8* (25), 6689-6692.
16. Faul M, X. L., Wald MM, Coronado VG. *Atlanta (GA): Centers for Disease Control and Prevention, National Center for Injury Prevention and Control* **2010**.
17. *MMWR Morb Mortal Wkly Rep* **2013,** (62), 549-52.
18. Werner, C.; Engelhard, K. *Br J Anaesth* **2007,** *99* (1), 4-9.
19. Wright, D. W.; Yeatts, S. D.; Silbergleit, R.; Palesch, Y. Y.; Hertzberg, V. S.; Frankel, M.; Goldstein, F. C.; Caveney, A. F.; Howlett-Smith, H.; Bengelink, E. M.; Manley, G. T.; Merck, L. H.; Janis, L. S.; Barsan, W. G. *N Engl J Med* **2014,** *371* (26), 2457-2466.
20. Wright, D. W.; Kellermann, A. L.; Hertzberg, V. S.; Clark, P. L.; Frankel, M.; Goldstein, F. C.; Salomone, J. P.; Dent, L. L.; Harris, O. A.; Ander, D. S.; Lowery, D. W.; Patel, M. M.; Denson, D. D.; Gordon, A. B.; Wald, M. M.; Gupta, S.; Hoffman, S. W.; Stein, D. G. *Ann Emerg Med* **2007,** *49* (4), 391-402.e2.
21. Palmer, T. D.; Willhoite, A. R.; Gage, F. H. *J Comp Neurol* **2000,** *425* (4), 479-494.
22. Chodobski, A.; Chung, I.; Koźniewska, E.; Ivanenko, T.; Chang, W.; Harrington, J. F.; Duncan, J. A.; Szmydynger-Chodobska, J. *Neuroscience* **2003,** *122* (4), 853-867.
23. Krum, J. M.; Mani, N.; Rosenstein, J. M. *Neuroscience* **2002,** *110* (4), 589-604.
24. Morgan, R.; Kreipke, C. W.; Roberts, G.; Bagchi, M.; Rafols, J. A. *Neurol Res* **2007,** *29*, 375-381.
25. Miller, M. S. *J Foot Ankle Surg* **1999,** *38* (3), 227-231.
26. Steed, D. L.; Study Group *, t. D. U. *J Vasc Surg* **1995,** *21* (1), 71-81.
27. Xiong, Y.; Mahmood, A.; Chopp, M. *Curr Opin Investig Drugs* **2010,** *11* (3), 298-308.
28. Risau, W. *Nature* **1997,** *386* (6626), 671-4.
29. Otrock, Z. K.; Mahfouz, R. A. R.; Makarem, J. A.; Shamseddine, A. I. *Blood Cell. Mol. Dis.* **2007,** *39* (2), 212-220.

30. Ausprunk, D. H.; Folkman, J. *Microvasc Res* **1977,** *14* (1), 53-65.
31. Vailhe, B.; Vittet, D.; Feige, J.-J. *Lab. Invest.* **2001,** *81* (4).
32. Hyder, S. M.; Stancel, G. M. *Molecular Endocrinology* **1999,** *13* (6), 806-811.
33. Ausprunk, D. H.; Folkman, J. *Microvascular Research* **1977,** *14* (1), 53-65.
34. Pandya, N. M.; Dhalla, N. S.; Santani, D. D. *Vasc. Pharmacol.* **2006,** *44* (5), 265-274.
35. Shestenko, O. P.; Nikonov, S. D.; Mertvetsov, N. P. *Mol Biol*

2001, *35* (3), 294-314.
36. Fagiani, E.; Christofori, G. *Cancer Lett* **2013,** *328* (1), 18-26.
37. Wang, D.; DuBois, R. N. *Proc Natl Acad Sci U S A* **2004,** *101* (2), 415-416.
38. Cheng, N.; Brantley, D. M.; Chen, J. *Cytokine Growth Factor Rev* **2002,** *13* (1), 75-85.
39. Zhang, X.; Ibrahimi, O. A.; Olsen, S. K.; Umemori, H.; Mohammadi, M.; Ornitz, D. M. *J Biol Chem* **2006,** *281* (23), 15694-15700.
40. Oh, I.; Kim, H. *Biotechnol Bioprocess Eng* **2004,** *9* (3), 201-206.
41. Cooke, M., John P.; Dzau, M., Victor J. *Annu Rev Med* **1997,** *48* (1), 489-509.
42. Le Tourneau, T.; Van Belle, E.; Corseaux, D.; Vallet, B. t.; Lebuffe, G.; Dupuis, B.; Lablanche, J.-M.; McFadden, E.; Bauters, C.; Bertrand, M. E. *J Am Coll Cardiol* **1999,** *33* (3), 876-882.
43. Szabó, C.; Papapetropoulos, A. *Br J Pharmacol* **2011,** *164* (3), 853-865.
44. Cianfarani, F.; Tommasi, R.; Failla, C. M.; Viviano, M. T.; Annessi, G.; Papi, M.; Zambruno, G.; Odorisio, T. *Br J Dermatol* **2006,** *154* (1), 34-41.
45. Van Belle, E.; Witzenbichler, B.; Chen, D.; Silver, M.; Chang, L.; Schwall, R.; Isner, J. M. *Circulation* **1998,** *97* (4), 381-390.
46. Greenhalgh, D. G.; Spruge, K. H.; Murray, M. J.; Ross, R. *Am J Pathol* **1990,** *136* (6), 1235-1246.
47. Stupack, D. G.; Cheresh, D. A., Integrins and Angiogenesis. In *Curr Top Dev Biol*, Academic Press: 2004; Vol. Volume 64, pp 207-238.
48. Ferrari, G.; Cook, B. D.; Terushkin, V.; Pintucci, G.; Mignatti, P. *J Cell Physiology* **2009,** *219* (2), 449-458.
49. Holmes, D.; Zachary, I. *Genome Biol* **2005,** *6* (2), 209.
50. Otrock, Z. K.; Makarem, J. A.; Shamseddine, A. I. *Blood Cells Mol Dis* **2007,** *38* (3), 258-268.
51. Otrock, Z. K.; Mahfouz, R. A. R.; Makarem, J. A.; Shamseddine, A. I. *Blood Cells Mol Dis* **2007,** *39* (2), 212-220.
52. Ferrara, N.; Gerber, H.; LeCouter, J. *Nat Med* **2003,** *9* (6), 667-76.
53. Thau-Zuchman, O.; Shohami, E.; Alexandrovich, A. G.; Leker, R. R. *Neuroscience* **2012,** *202* (0), 334-341.
54. Jakeman, L. B.; M., A.; S., P. H.; Ferrara, N. *Endocrinology* **1993,** *133* (2), 848-859.
55. Coultas, L.; Chawengsaksophak, K.; Rossant, J. *Nature* **2005,** *438* (7070), 937-945.
56. Hyder, S. M.; Stancel, G. M. *Mol Endocrinol* **1999,** *13* (6), 806-811.
57. Carmeliet, P.; Ferreira, V.; Breier, G.; Pollefeyt, S.; Kieckens, L.; Gertsenstein, M.; Fahrig, M.; Vanddenhoeck, A.; Harpal, K.; Eberhardt, C.; Declercq, C.; Pawling, L.; Collen, D.; Risau, W.; NAgy, A. *Nature* **1996,** *380* (6573), 435-439.
58. Hiratsuka, S.; Nakamura, K.; Iwai, S.; Murakami, M.; Itoh, T.; Kijima, H.; Shipley, J. M.; Senior, R. M.; Shibuya, M. *Cancer Cell* **2002,** *2* (4), 289-300.
59. Facchiano, A.; Russo, K.; Facchiano, A. M.; De Marchis, F.; Facchiano, F.; Ribatti, D.; Aguzzi, M. S.; Capogrossi, M. C. *J Biol Chem* **2003,** *278* (10), 8751-8760.
60. Comerota, A. J.; Throm, R. C.; Miller, K. A.; Henry, T.; Chronos, N.; Laird, J.; Sequeira, R.; Kent, C. K.; Bacchetta, M.; Goldman, C.; Salenius, J.-P.; Schmieder, F. A.; Pilsudski, R. *J Vasc Surg* **2002,** *35* (5), 930-936.
61. Lindahl, P.; Johansson, B. R.; Levéen, P.; Betsholtz, C. *Science* **1997,** *277* (5323), 242-245.
62. Bouïs, D.; Kusumanto, Y.; Meijer, C.; Mulder, N. H.; Hospers, G. A. P. *Pharmacol Res* **2006,** *53* (2), 89-103.

63. Bennett, S. P.; Griffiths, G. D.; Schor, A. M.; Leese, G. P.; Schor, S. L. *Br J Surg* **2003,** *90* (2), 133-146.
64. Wacker, B. K.; Alford, S. K.; Scott, E. A.; Das Thakur, M.; Longmore, G. D.; Elbert, D. L. *Biophys J* **2008,** *94* (1), 273-285.
65. Goodman, S. L.; Deutzmann, R.; von der Mark, K. *J Cell Biol* **1987,** *105* (1), 589-598.
66. Aumailley, M.; Nurcombe, V.; Edgar, D.; Paulsson, M.; Timpl, R. *J Biol Chem* **1987,** *262* (24), 11532-11538.
67. Yamada, M.; Kadoya, Y.; Kasai, S.; Kato, K.; Mochizuki, M.; Nishi, N.; Watanabe, N.; Kleinman, H. K.; Yamada, Y.; Nomizu, M. *FEBS Lett* **2002,** *530* (1–3), 48-52.
68. Pierschbacher, M. D.; Ruoslahti, E. *Nature* **1984,** *309* (5963), 30-33.
69. Santoro, S. A. *Cell* **1986,** *46* (6), 913-920.
70. Kramer, R. H.; Marks, N. *J Biol Chem* **1989,** *264* (8), 4684-4688.
71. Courter, D.; Cao, H.; Kwok, S.; Kong, C.; Banh, A.; Kuo, P.; Bouley, D. M.; Vice, C.; Brustugun, O. T.; Denko, N. C.; Koong, A. C.; Giaccia, A.; Le, Q.-T. *PLoS ONE* **2010,** *5* (3), e9633.
72. Oldberg, A.; Franzén, A.; Heinegård, D. *Proc Natl Acad Sci U S A* **1986,** *83* (23), 8819-8823.
73. Schvartz, I.; Seger, D.; Shaltiel, S. *Int J Biochem Cell Biol* **1999,** *31* (5), 539-544.
74. Jang, J.-H.; Hwang, J.-H.; Chung, C.-P. *Biotechnol Lett* **2004,** *26* (24), 1831-1835.
75. Murphy-Ullrich, J. E. *J Clin Invest* **2001,** *107* (7), 785-790.
76. Mohri, H.; Hashimoto, Y.; Ohba, M.; Kumagai, H.; Ohkubo, T. *Am J Hematol* **1991,** *37* (1), 14-19.
77. Lee, D.-E.; Hong, Y.-D.; Choi, K.-H.; Lee, S.-Y.; Park, P.-H.; Choi, S.-J. *Appl Radiat Isot* **2010,** *68* (10), 1896-1902.
78. Taite, L. J.; Yang, P.; Jun, H.-W.; West, J. L. *J Biomed Mater Res B Appl Biomater* **2008,** *84B* (1), 108-116.
79. Jun, H.-W.; West, J. L. *J Biomed Mater Res B Appl Biomater* **2005,** *72B* (1), 131-139.
80. Yokosaki, Y.; Matsuura, N.; Sasaki, T.; Murakami, I.; Schneider, H.; Higashiyama, S.; Saitoh, Y.; Yamakido, M.; Taooka, Y.; Sheppard, D. *J Biol Chem* **1999,** *274* (51), 36328-36334.
81. Senger, D. R.; Ledbetter, S. R.; Claffey, K. P.; Papadopoulos-Sergiou, A.; Peruzzi, C. A.; Detmar, M. *Am J Pathol* **1996,** *149* (1), 293-305.
82. Hamada, Y.; Egusa, H.; Kaneda, Y.; Hirata, I.; Kawaguchi, N.; Hirao, T.; Matsumoto, T.; Yao, M.; Daito, K.; Suzuki, M.; Yatani, H.; Daito, M.; Okazaki, M.; Matsuura, N. *Dent Mater J* **2007,** *26* (4), 487-492.
83. Hamada, Y.; Nokihara, K.; Okazaki, M.; Fujitani, W.; Matsumoto, T.; Matsuo, M.; Umakoshi, Y.; Takahashi, J.; Matsuura, N. *Biochem Biophys Res Commun* **2003,** *310* (1), 153-157.
84. Pisal, D. S.; Kosloski, M. P.; Balu-Iyer, S. V. *J Pharm Sci* **2010,** *99* (6), 2557-2575.
85. Polhemus, D. J.; Lefer, D. J. *Circ Res* **2014,** *114* (4), 730-737.
86. Mann, B. E.; Motterlini, R. *Chem Commun* **2007,** (41), 4197-4208.
87. Cortez, M. A.; Grayson, S. M. *Macromolecules* **2010,** *43* (9), 4081-4090.
88. Mathai, J. C.; Missner, A.; Kügler, P.; Saparov, S. M.; Zeidel, M. L.; Lee, J. K.; Pohl, P. *Proc Natl Acad Sci* **2009,** *106* (39), 16633-16638.
89. Otterbein, L. E.; Choi, A. M. K. *Am J Physiol Lung Cell Mol Physiol* **2000,** *279* (6), L1029-L1037.
90. Foresti, R.; Hammad, J.; Clark, J. E.; Johnson, T. R.; Mann, B. E.; Friebe, A.; Green, C. J.; Motterlini, R. *Br J Pharmacol* **2004,** *142* (3), 453-460.
91. Otterbein, L. E.; Bach, F. H.; Alam, J.; Soares, M.; Hong, T. L.; Wysk, M.; Davis, R. J.; Flavell, R. A.; Choi, A. M. K. *Nat Med* **2000,** *6* (4), 422-8.
92. Parfenova, H.; Basuroy, S.; Bhattacharya, S.; Tcheranova, D.; Qu, Y.; Regan, R. F.; Leffler, C. W. *Am J Physiol Cell Physiol* **2006,** *290* (5), 1399-1410.
93. Förstermann, U.; Closs, E. I.; Pollock, J. S.; Nakane, M.; Schwarz, P.; Gath, I.; Kleinert, H. *Hypertension* **1994,** *23* (6 Pt 2), 1121-31.

94. Masters, K. S. B.; Leibovich, S. J.; Belem, P.; West, J. L.; Poole-Warren, L. A. *Wound Repair Regen* **2002,** *10* (5), 286-294.
95. Hosoki, R.; Matsuki, N.; Kimura, H. *Biochem Biophys Res Commun* **1997,** *237* (3), 527-531.
96. Prast, H.; Philippu, A. *Prog Neurobiol* **2001,** *64* (1), 51-68.
97. Wang, R. *Physiol Rev* **2012,** *92* (2), 791-896.
98. Abe, K.; Kimura, H. *J Neurosci* **1996,** *16* (3), 1066-1071.
99. Paul, B. D.; Snyder, S. H. *Rev Mol Cell Biol* **2012,** *13* (8), 499-507.
100. Caliendo, G.; Cirino, G.; Santagada, V.; Wallace, J. L. *J Med Chem* **2010,** *53* (17), 6275-6286.
101. Shibuya, N.; Mikami, Y.; Kimura, Y.; Nagahara, N.; Kimura, H. *J Biochem* **2009,** *146* (5), 623-626.
102. Tanizawa, K. *J Biochem* **2011,** *149* (4), 357-359.
103. Shibuya, N.; Tanaka, M.; Yoshida, M.; Ogasawara, Y.; Togawa, T.; Ishii, K.; Kimura, H. *Antioxid Redox Signal* **2009,** *11* (4), 703-714.
104. Papapetropoulos, A.; Pyriochou, A.; Altaany, Z.; Yang, G.; Marazioti, A.; Zhou, Z.; Jeschke, M. G.; Branski, L. K.; Herndon, D. N.; Wang, R.; Szabó, C. *Proc Natl Acad Sci* **2009,** *106* (51), 21972-21977.
105. Tao, B.-B.; Liu, S.-Y.; Zhang, C.-C.; Fu, W.; Cai, W.-J.; Wang, Y.; Shen, Q.; Wang, M.-J.; Chen, Y.; Zhang, L.-J.; Zhu, Y.-Z.; Zhu, Y.-C. *Antioxid Redox Signal* **2012,** *19* (5), 448-464.
106. Whiteman, M.; Moore, P. K. *J Cell Mol Med* **2009,** *13* (3), 488-507.
107. Wallace, J. L. *Trends Pharmacol Sci* **2007,** *28* (10), 501-505.
108. Zhao, Y.; Wang, H.; Xian, M. *J Am Chem Soc* **2010,** *133* (1), 15-17.
109. Martelli, A.; Testai, L.; Citi, V.; Marino, A.; Pugliesi, I.; Barresi, E.; Nesi, G.; Rapposelli, S.; Taliani, S.; Da Settimo, F.; Breschi, M. C.; Calderone, V. *ACS Med Chem Lett* **2013,** *4* (10), 904-908.
110. Foster, J. C.; Powell, C. R.; Radzinski, S. C.; Matson, J. B. *Org Lett* **2014,** *16* (6), 1558-1561.
111. Hasegawa, U.; van der Vlies, A. J. *Bioconjug Chem* **2014**.
112. Foster, J. C.; Matson, J. B. *Macromolecules* **2014**.
113. Berndt, P.; Fields, G. B.; Tirrell, M. *J Am Chem Soc* **1995,** *117* (37), 9515-9522.
114. Cui, H.; Webber, M. J.; Stupp, S. I. *Biopolymers* **2010,** *94* (1), 1-18.
115. Gazit, E. *FASEB J* **2002,** *16* (1), 77-83.
116. Jayawarna, V.; Ali, M.; Jowitt, T. A.; Miller, A. F.; Saiani, A.; Gough, J. E.; Ulijn, R. V. *Adv Mater* **2006,** *18* (5), 611-614.
117. Fleming, S.; Debnath, S.; Frederix, P. W. J. M.; Tuttle, T.; Ulijn, R. V. *Chem Commun* **2013,** *49* (90), 10587-10589.
118. Kendrew, J. C.; Dickerson, R. E.; Strandberg, B. E.; Hart, R. G.; Davies, D. R.; Phillips, D. C.; Shore, V. C. *Nature* **1960,** *185* (4711), 422-427.
119. Levitt, M. *Biochemistry* **1978,** *17* (20), 4277-4285.
120. Tsai, H.-H.; Gunasekaran, K.; Nussinov, R. *Structure* **2006,** *14* (6), 1059-1072.
121. Merrifield, R. B. *J Am Chem Soc* **1963,** *85* (14), 2149-2154.
122. Rivard, A.; Fabre, J.-E.; Silver, M.; Chen, D.; Murohara, T.; Kearney, M.; Magner, M.; Asahara, T.; Isner, J. M. *Circulation* **1999,** *99* (1), 111-120.
123. Martin, A.; Komada, M. R.; Sane, D. C. *Med Res Rev* **2003,** *23* (2), 117-145.
124. Bauer, S. M.; Bauer, R. J.; Velazquez, O. C. *Vasc Endovascular Surg* **2005,** *39* (4), 293-306.
125. Folkman, J.; Shing, Y. *J Biol Chem* **1992,** *267* (16), 10931-10934.
126. Lazarous, D. F.; Unger, E. F.; Epstein, S. E.; Stine, A.; Arevalo, J. L.; Chew, E. Y.; Quyyumi, A. A. *J Am Coll Cardiol* **2000,** *36* (4), 1239-1244.
127. FDA announces new labeling changes for Regranex [news release] http://www.fda.gov/bbs/topics/NEWS/2008/NEW01845.html. (accessed June 10, 2008).
128. Lee, K.; Silva, E. A.; Mooney, D. J. *J R Soc Interface* **2011,** *8* (55), 153-170.
129. Sodek, J.; Ganss, B.; McKee, M. D. *Crit Rev Oral Biol Med* **2000,** *11* (3), 279-303.
130. Barry, S. T.; Ludbrook, S. B.; Murrison, E.; Horgan, C. M. T. *Exp Cell Res* **2000,** *258* (2), 342-351.

131. Park, K. M.; Lee, Y.; Son, J. Y.; Bae, J. W.; Park, K. D. *Bioconjug Chem* **2012,** *23* (10), 2042-2050.
132. Greenfield, M. A.; Hoffman, J. R.; Olvera de la Cruz, M.; Stupp, S. I. *Langmuir* **2009,** *26* (5), 3641-3647.
133. Niles, A. L.; Moravec, R. A.; Eric Hesselberth, P.; Scurria, M. A.; Daily, W. J.; Riss, T. L. *Anal Biochem* **2007,** *366* (2), 197-206.
134. Fukuto, J. M.; Carrington, S. J.; Tantillo, D. J.; Harrison, J. G.; Ignarro, L. J.; Freeman, B. A.; Chen, A.; Wink, D. A. *Chem Res Toxicol* **2012,** *25* (4), 769-793.
135. Paul, B. D.; Sbodio, J. I.; Xu, R.; Vandiver, M. S.; Cha, J. Y.; Snowman, A. M.; Snyder, S. H. *Nature* **2014,** *509* (7498), 96-100.
136. Polhemus, D. J.; Calvert, J. W.; Butler, J.; Lefer, D. J. *Scientifica* **2014,** *2014*, 8.
137. Peng, B.; Chen, W.; Liu, C.; Rosser, E. W.; Pacheco, A.; Zhao, Y.; Aguilar, H. C.; Xian, M. *Chem Eur J* **2014,** *20* (4), 1010-1016.
138. Montoya, L. A.; Pluth, M. D. *Chem Commun* **2012,** *48* (39), 4767-4769.
139. Stasko, N. A.; Schoenfisch, M. H. *J Am Chem Soc* **2006,** *128* (25), 8265-8271.
140. Kapadia, M. R.; Chow, L. W.; Tsihlis, N. D.; Ahanchi, S. S.; Eng, J. W.; Murar, J.; Martinez, J.; Popowich, D. A.; Jiang, Q.; Hrabie, J. A.; Saavedra, J. E.; Keefer, L. K.; Hulvat, J. F.; Stupp, S. I.; Kibbe, M. R. *J Vasc Surg* **2008,** *47* (1), 173-182.
141. Hasegawa, U.; van der Vlies, A. J.; Simeoni, E.; Wandrey, C.; Hubbell, J. A. *J Am Chem Soc* **2010,** *132* (51), 18273-18280.
142. Allan, P. K.; Wheatley, P. S.; Aldous, D.; Mohideen, M. I.; Tang, C.; Hriljac, J. A.; Megson, I. L.; Chapman, K. W.; De Weireld, G.; Vaesen, S.; Morris, R. E. *Dalton Trans* **2012,** *41* (14), 4060-4066.
143. Marshall, N. J.; Goodwin, C. J.; Holt, S. J. *Growth Regul* **1995,** *5* (2), 69-84.
144. Cory, A.; Owen, T.; Barltrop, J.; Cory, J. *Cancer Commun* **1991,** *3* (7), 207-12.
145. Hartgerink, J. D.; Beniash, E.; Stupp, S. I. *Science* **2001,** *294* (5547), 1684-1688.
146. Pashuck, E. T.; Cui, H.; Stupp, S. I. *J Am Chem Soc* **2010,** *132* (17), 6041-6046.
147. Carlson, K. L.; Lowe, S. L.; Hoffmann, M. R.; Thomasson, K. A. *J Phys Chem A* **2005,** *109* (24), 5463-5470.
148. Greenfield, N. J. *Nat protoc* **2006,** *1* (6), 2876-2890.
149. Ganim, Z.; Chung, H. S.; Smith, A. W.; DeFlores, L. P.; Jones, K. C.; Tokmakoff, A. *Acc Chem Res* **2008,** *41* (3), 432-441.
150. Barth, A.; Zscherp, C. *Q Rev Biophys* **2002,** *35* (4), 369-430.
151. Liu, C.; Pan, J.; Li, S.; Zhao, Y.; Wu, L. Y.; Berkman, C. E.; Whorton, A. R.; Xian, M. *Angew Chem Int Ed Engl* **2011,** *50* (44), 10327-10329.
152. Lambert, D. M.; Vandevoorde, S.; Diependaele, G.; Govaerts, S. J.; Robert, A. R. *Epilepsia* **2001,** *42* (3), 321-327.
153. Calignano, A.; Rana, G. L.; Giuffrida, A.; Piomelli, D. *Nature* **1998,** *394* (6690), 277-281.
154. Lo Verme, J.; Fu, J.; Astarita, G.; La Rana, G.; Russo, R.; Calignano, A.; Piomelli, D. *Mol Pharmacol* **2005,** *67* (1), 15-19.
155. Hesselink, J. M. K.; Hekker, T. A. M. *J Pain Res* **2012,** *5*, 437-442.

APPENDIX

A. Other Syntheses

i. Synthesis of palmitoylethanolamide (PEA)

The inhibitor MeHQ was removed from vinyl palmitate (VP) by passing it through an aluminum oxide column (activated, neutral, Brockman I). Due to the high freezing point (22 °C) of VP, it was allowed to warm up before handling. Methanol (3mL) was used to dissolve ethanolamine (4.28 mL) in a round bottom flask at 60 °C for 5 min. The VP (1 g) was introduced and the reaction was stirred under N_2 at rt. The clear reaction mixture began turning into a white viscous mixture over the duration of 2 h. The excess ethanolamine was removed by filtration. The crude product was washed via DI water filtrations (18 mL 3X) and allowed to dry at rt overnight. To remove the impurities and byproducts (*N*-*O*-bis-palmitolyethanolamine and potentially *O*-palmitoylethanolamine) the crude product was further purified by trituration first adding 50 mL of DCM followed by 50 mL of chloroform. The product was recovered by filtration and analyzed by NMR. ^{1}H NMR ($CDCl_3$): δ 0.89 (t, 3H), 1.26 (s, 24H), 1.65 (m, 2H), 2.21 (t, 2H), 3.45 (q, 2H), 3.74 (t, 2H).

ii. Synthesis of ABA-IAVE$_3$

Rink amide MBHA resin (100-200 mesh; 0.48 mmol/g) was weighed into a reaction vessel. The resin was allowed to swell in dichloromethane (DCM) (10 mL) for 20 min prior to loading the first amino acid. A deprotection solution of 2% piperidine and 2% DBU in *N*,*N*-

dimethylformamide (DMF) was used to remove the N-terminal Fmoc. 10 mL of this solution was added to the reaction vessel and the reaction mixture was agitated for 5 min. The solution was removed and this step was repeated once more. The resin was washed with DCM (3 x 5 mL) and DMF (3 x 5 mL). A coupling solution of amino acid (4 equiv), *N*,*N*,*N*,*N*-tetramethyl-*O*-(1H-benzotriazol-1-yl)uranium hexafluorophosphate (HBTU) (3.9 equiv), and *N*,*N*-diisopropylethylamine (DIEA) (0.6 mL, 6 equiv) dissolved in 15 mL of DMF was added to the reaction vessel containing the resin, and the suspension was agitated for 2 h. The solution was drained, and the resin was washed with DCM (3 x 5 mL) and DMF (3 x 5 mL). This procedure was repeated for each coupling step. After deprotection of the last amino acid (Ile), the linker, 4-acetylbenzoic acid (ABA) (4 equiv), was introduced using standard amino acid coupling procedures as described above. Once the linker was successfully coupled to the peptide, the peptide was cleaved from the resin by treatment with trifluoroacetic acid (TFA)/H_2O (97:3) for 2 h under constant agitation. The cleavage solution containing the peptide was drained into a 250-mL round bottom flask, and the resin was washed with DCM (2 x 10 mL). The combined cleavage solution and washes were concentrated to 2 mL via rotary evaporation, and then diethyl ether was added to precipitate out the peptide. The crude peptide was recovered via vacuum filtration, allowed to dry, stored at 4^{o}C until HPLC purification. To dissolve the peptide after cleavage, 0.1% NH_4OH in milliQ water was added and concentrated NH_4OH was added drop-wise to adjust the pH to 8. The solution was passed through a 0.22 mm filter prior to HPLC purification.

iii. Synthesis of SATO-ABA-IAVE$_3$

To a solution of ABA-IAVE$_3$ (15 mg) in 4:6/HFIP:DCM (250 μL) was added *S*--benzoylthiohydroxylamine (4 equiv). TFA (3 equiv) and was added to the solution, as a catalyst. After 2 hr, the solvent mixture was lyophilized under high vacuum. Once dry, the product was stored in the freezer until purification. Just before purification, the crude product was taken up in 0.01% NH_4OH milliQ water, which afforded an aqueous solution at pH ~7. This solution was passed through a 0.22 mm filter prior to HPLC purification.